Contributions to Zoology, 87 (4) 197-225 (2018)

Disentangling a cryptic species complex and defining new species within the *Eumerus minotaurus* group (Diptera: Syrphidae), based on integrative taxonomy and Aegean palaeogeography

Antonia Chroni[1,4,5], Ana Grković[2], Jelena Ačanski[3], Ante Vujić[2], Snežana Radenković[2], Nevena Veličković[2], Mihajla Djan[2], Theodora Petanidou[1]

[1] *University of the Aegean, Department of Geography, University Hill, 81100, Mytilene, Greece*
[2] *University of Novi Sad, Faculty of Sciences, Department of Biology and Ecology, Trg Dositeja Obradovića 2, 21000, Novi Sad, Serbia*
[3] *Laboratory for Biosystems Research, BioSense Institute – Research Institute for Information Technologies in Biosystems, University of Novi Sad, Dr. Zorana Đinđića 1, 21000, Novi Sad, Serbia*
[4] *Institute for Genomics and Evolutionary Medicine; Department of Biology, Temple University, Philadelphia, PA 19122, USA*
[5] *E-mail: tonichr3@gmail.com*

Keywords: Aegean, DNA sequences, hoverflies, mid-Aegean Trench, wing geometric morphometry

Abstract

This study provides an overview of the *Eumerus minotaurus* taxon group, diagnosing a new species, *E. anatolicus* Grković, Vujić and Radenković sp. n. (Muğla, Turkey), and unraveling three cryptic species within *E. minotaurus*: *E. karyates* Chroni, Grković and Vujić sp. n. (Peloponnese, Greece), *E. minotaurus* Claussen and Lucas, 1988 (Crete and Karpathos, Greece) and *E. phaeacus* Chroni, Grković and Vujić sp. n. (Corfu and Mt Olympus, Greece; Mt Rumija, Montenegro). We applied an integrative taxonomic approach based on molecular, morphological and wing geometric morphometric data to corroborate and delimit cryptic species within the complex. In addition, we discuss the latent biogeographic patterns and speciation processes leading to configuration of the *E. minotaurus* group based on palaeogeographic evolution of the Aegean. Mitochondrial phylogeographic analysis suggested that speciation within the *E. minotaurus* group is attributable to formation of the mid-Aegean Trench and Messinian Salinity Crisis, and was integrated at the Pleistocene. We show that more accurate estimates of divergence times may be based on geological events rather than the standard arthropod mtDNA substitution rate.

Contents

Introduction

Integrative taxonomy is a multisource approach that takes advantage of complementarity among disciplines and tends to gain ground more and more in species delimitation and diagnosis of cryptic diversity (Dayrat, 2005; Padial *et al*., 2010; Schlick-Steiner *et al*., 2010). Single-method approaches in taxonomic and systematic studies have many limitations, especially for diagnosis of cryptic species and, as a result, (two or more) distinct species are often erroneously classified (and hidden) under one species name (Bickford *et al*., 2007; Pfenninger and Schwenk, 2007). Cryptic species are morphologically indistinguishable but genetically distinct lineages, so a combination of molecular, biological and morphological approaches, as well as phylogeographic and population genetic analyses have been proposed (and are required) as a framework to diagnose and distinguish cryptic species (Pérez-Ponce de León and Nadler, 2010). Mitochondrial (DNA barcodes; Hebert *et al*., 2003) and nuclear molecular markers (*e.g*. 28S, Belshaw *et al*., 1998) have contributed to tally up the total species diversity, leading to the prosperity of integrative taxonomy (*e.g*.

hoverflies, Mengual *et al*., 2008) and the detection of new species (beetles, Soldati *et al*., 2014; butterflies, Kirichenko *et al*., 2015; cone snails, Puillandre *et al*., 2014; flies, Diaz *et al*., 2015) as well as cryptic species complexes (earthworms, Martinsson and Erséus, 2017; flies, Dias *et al*., 2016; Šašić *et al*., 2016; lizards, Rato *et al*., 2016; plants, Perez *et al*., 2016; rotifers, Papakostas *et al*., 2016).

The hoverfly genus *Eumerus* Meigen, 1822 (Diptera: Syrphidae) accounts of its great diversity (256 species recorded worldwide, Pape and Thompson, 2015, of which 37 occur in southeastern Europe, Grković *et al*., 2017), yet we know little about its fauna (unknown total species number as *e.g*. new species are regularly described: Doczkal, 1996; Speight *et al*., 2013; Grković *et al*., 2015, 2017; Markov *et al*., 2016), habitat preferences (Speight, 2016), life cycle (often strictly connected to plant species, Arzone, 1971, 1973; Pérez-Bañón and Marcos-García, 1998; Speight, 2016) or foraging behaviour (pests of vegetables, Doczkal, 1996; Pérez-Bañón and Marcos-García, 1998; flower visitors, Petanidou *et al*., 2011; Speight, 2016). In addition, the nomenclatural history and the taxonomic statuses within the genus are complex and unclear, highlighting the need to revise the genus' taxonomy. Considering the importance of hoverflies in ecosystems (as pollinators, predators of plant pests, herbivores, etc.; Rotheray and Gilbert, 2011), further ecological and biogeographic studies are needed; there might be more out there that we are missing which should be taken into account in, *e.g*. conservation outlines.

Heretofore, few studies have tackled unresolved problems of the genus *Eumerus* with DNA barcoding, let alone integrative taxonomy being employed. New species, some of them endemics, have been described over the past decade (Doczkal, 1996; Ricarte *et al*., 2012; Grković *et al*., 2015, 2017; Markov *et al*., 2016; van Steenis *et al*., 2017; Smit *et al*., 2017), and several taxon groups (hereafter named as 'groups') have been proposed within the genus (Chroni *et al*., 2017). The latter study suggested the configuration of the *Eumerus minotaurus* group with two related species: *E. crassus* Grković, Vujić and Radenković, 2015 (species range: Lesvos Island, Greece; originally identified as *E. niehuisi* Doczkal, 1996, and treated as such in the respective publication; specimen EU37) and *E. minotaurus* Claussen and Lucas, 1988 (species range: Crete and Thessaly, Greece; and parts of the former Yugoslavia; Speight, 2016) (Figure 1A). Doczkal (1996) discussed this topic, and suggested an affinity for *E. longicornis* Loew, 1855 (species range requires confirmation, but probably: southern and central Germany, Slovakia, Hungary and the Mts Caucasus; Speight, 2016), *E. minotaurus*, *E. niehuisi* (species range: Corsica and Sardinia; Doczkal, 1996) and *E. sibiricus* Stackelberg, 1952 (species range: Siberia; drawn by Stackelberg, 1961; Doczkal, 1996; Figure 1B). Within the frame of this study, we considered all aforementioned species (Doczkal, 1996; Chroni *et al*., 2017) to belong to the *E. minotaurus* group (Figure 1C), and we studied the species and specimens (at our disposal) originating from southeastern Europe. We have employed an integrative approach that utilizes molecular, morphological and wing morphometric data (*E. crassus* and *E. minotaurus*) or morphological data alone due to unavailability of DNA sequences (*E. longicornis*). Our current analyses denoted a cryptic species complex within *E. minotaurus* and one new species within the *E. minotaurus* group. Cryptic diversity is frequently encountered among hoverflies, with examples described for the genera *Chrysotoxum* (Nedeljković *et al*., 2013, 2015), *Merodon* (*M. aureus* group, Šašić *et al*., 2016; *M. avidus*, Popović *et al*., 2015, Ačanski *et al*., 2016; *M. nanus* group, Vujić *et al*., 2014), *Microdon* (*M. myrmicae*, Bonelli *et al*., 2011) and *Pipiza* (Vujić *et al*., 2013).

The Aegean archipelago and its adjacent regions (Balkan Peninsula, Greek mainland and Anatolian coast) are well-known for their high diversity of both cryptic and endemic species (Poulakakis *et al*., 2015), as well as for the multiple and complex alterations that have occurred from the Miocene (23 Mya) through to the Holocene (0.0117 Mya to the present) (Poulakakis *et al*., 2015; Gkontas *et al*., 2016; Kougioumoutzis *et al*., 2017; Sfenthourakis and Triantis, 2017). Four major geological events in the Aegean region are considered liable for significant species dispersal barriers: (1) formation of the mid-Aegean Trench (MAT) in the middle Miocene (12-9 Mya), during which a sea interference separated eastern from central-western regions (Sfenthourakis and Triantis, 2017); (2) isolation of Crete from the Peloponnese (5.5-5 Mya) after the Messinian Salinity Crisis (MSC) in the late Miocene (5.96-5.33 Mya) when the Mediterranean Sea almost desiccated allowing every species to travel anywhere wanted; (3) extensive segregation and widening of the Aegean Sea and separation of the Karpathos–Kassos island group from Rhodos in the Pliocene (5-2 Mya); and (4) orogenetic and eustatic sea-level changes during the Pleistocene (2-0.0117 Mya) (Kougioumoutzis *et al*., 2017; Sfenthourakis and Triantis, 2017). A series of phenomena including geological (geotectonic forces) and climatic events (sea-level oscillations) as well as

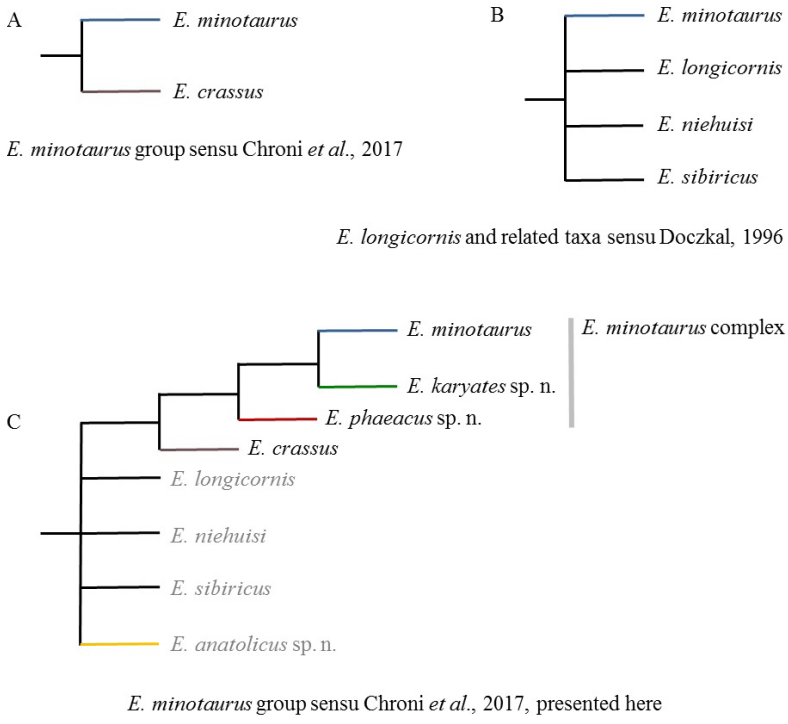

Figure 1. Species composition for (A) the *E. minotaurus* group sensu Chroni *et al*., 2017; (B) *E. longicornis* and related taxa sensu Doczkal, 1996; and (C) the *E. minotaurus* group sensu Chroni *et al*., 2017 presented here (species in grey were not included in integrative taxonomy approach due to unavailability of DNA sequences). The branches of species discussed in the present study are marked with different colours: *E. anatolicus* sp. n. (orange), *E. crassus* (grey), *E. karyates* sp. n. (green), *E. minotaurus* (blue) and *E. phaeacus* sp. n. (red) (for interpretation of the references to colour in this figure legend, the reader is asked to refer to the web version of this article).

human pressure (first evidence of human settlement in the Palaeolithic, ca. 130 000 years ago, Strasser *et al*., 2010), have shaped everything as known today, with the configuration or isolation of landmasses allowing or impeding the dispersal of organisms and thereby driving speciation or species extinction (Poulakakis *et al*., 2005; Parmakelis *et al*., 2006; Poulakakis and Sfenthourakis, 2008; Akin *et al*., 2010; Simaiakis *et al*., 2012; Gkontas *et al*., 2016; Sfenthourakis and Triantis, 2017).

The aims of our study were threefold: (a) to define and delimit cryptic species within *E. minotaurus* by integrating molecular markers (mtDNA and nDNA), subtle morphological characters and wing geometric morphometrics; (b) to provide an overview of the species within the *E. minotaurus* group and to explore the existence of new species within it; and (c) to investigate speciation processes and suggest a biogeographic pattern for the *E. minotaurus* group.

Material and methods

Specimen collection and morphological analysis

Our study relies on collections assembled by hand net between the years 2003 and 2016, and deposited in the entomological collections of the Faculty of Sciences of Novi Sad (FSUNS), the Melissotheque of the Aegean (University of the Aegean, Mytilene, Greece, MAegean) and the Finnish Museum of Natural History (Zoological Museum, Helsinki, Finland, MZH). The specimens of *E. anatolicus* sp. n. were collected by Malaise trap and belong to the Miroslav Barták collection (Faculty of Agrobiology, Food and Natural Resources, Czech University of Life Sciences, Prague). A total of 52 specimens from 19 species of *Eumerus*, representing 33 sampling localities, were used for the molecular analyses (Figure 2; Table 1; 15 specimens of representative *Eumerus* species and 37 of the *E. minotaurus* group. Sample sizes and provenances of the studied *E. minotaurus* group specimens used for morphological/molecular/wing morphometry analyses were, respectively (Figure 2): *E. crassus* (Greece: Chios, Evros, Lesvos, Mt Rhodope, Samos, Thassos; Turkey: Mt Bozdag; 40/4/10 specimens), *E. anatolicus* sp. n. (Turkey: Muğla; 7/-/- specimens), *E. karyates* sp. n. (Greece: Peloponnese; 8/8/9 specimens), *E. minotaurus* (Greece: Crete, Karpathos; 11/7/10 specimens) and *E. phaeacus* sp. n. (Greece: Corfu, Mt Olympus; Montenegro: Mt Rumija; 24/18/22 specimens). Additional material of representative *Eumerus* species from four countries was used in the molecular analyses (see Appendix for details). Furthermore, we examined two paratypes of *E. minotaurus* from the Zoological

Table 1. List of the specimens used for the molecular analyses, their locality information, and GenBank accession numbers. GenBank accession numbers of sequences: newly-generated (this study) are in boldface; previously-generated are in normal text; and retrieved from GenBank are in italics. FSUNS: Faculty of Sciences of Novi Sad, Serbia. MAegean: The Melissotheque of the Aegean, University of the Aegean, Mytilene, Greece. MZH: Finnish Museum of Natural History, Zoological Museum, Helsinki, Finland.

Sequence ID	Specimen voucher	3'-end fragment of COI	5'-end fragment of COI	28S	Species name	Species group	Species subgroup	Sex	Field data
EU10	FSUNS:G1147	**KY865493**	KX083349	none	*Eumerus alpinus* Rondani, 1857	*E. alpinus*	none	F	Italy, Toscana, Mts Apuane, near OrtoBotanico, 44.056359, 10.19884
EU132	FSUNS:60653	**KY865499**	KX083380	none	*Eumerus strigatus* (Fallen, 1817)	*E. strigatus*	none	M	Germany, Unknown
EU135	FSUNS:G3018	**KY865500**	**KY865450**	none	*Eumerus tricolor* (Fabricius), 1798	*E. tricolor*	none	F	Italy, Baragazza, 44.13217, 11.19112, 09/06/2013
EU146	FSUNS (loan by Maegean):E0787, UOTA_MEL026180	**KY865501**	**KY865451**	**KY865546**	*Eumerus minotaurus* Claussen & Lucas, 1988	*E. minotaurus*	*E. minotaurus*	M	Greece, Karpathos, Avlona, 35.7689, 27.1849, 2-4/05/2012
EU149	FSUNS:G3025	**KY865502**	**KY865452**	none	*Eumerus crassus* Grković, Vujić & Radenković, 2015	*E. minotaurus*	none	M	Greece, Chios, Kambia Gorge, 38.578499, 25.979666, 14/05/2009
EU16	FSUNS:G0278	**KY865494**	**KY865446**	**KY865545**	*Eumerus phaeacus* Chroni, Grković & Vujić, sp. n.	*E. minotaurus*	*E. minotaurus*	M	Greece, Mt Olympus, Ag. Paraskevi, kanjon, 39.8785, 22.5863, 17/05/2011
EU17	MAegean:UOTA_MEL0746, E0746	KT221020	KT221006	none	*Eumerus torsicus* Grković et Vujić, 2016	*torsicus*	none	M	Greece, Chios, Elinda, 38.393, 25.9914, 9-11/11/2012
EU211	FSUNS:G0277	**KY865503**	**KY865453**	**KY865550**	*Eumerus phaeacus* Chroni, Grković & Vujić, sp. n.	*E. minotaurus*	*E. minotaurus*	F	Greece, Mt Olympus, Ag. Paraskevi, kanjon, 39.8785, 22.5863, 17/05/2011
EU212	FSUNS:G0269	**KY865504**	**KY865454**	none	*Eumerus phaeacus* Chroni, Grković & Vujić, sp. n.	*E. minotaurus*	*E. minotaurus*	M	Montenegro, Mt Rumija, okosredine (deokajezeru, uz put), 42.11201, 19.21739, 02/05/2011
EU221	FSUNS:G0271	**KY865505**	**KY865455**	none	*Eumerus sinuatus* Loew, 1855	*E.tricolor*	none	M	Serbia, Fruska Gora, Glavica, 45.153999, 19.834681, 17/06/2011
EU223	FSUNS:G1020	**KY865506**	**KY865456**	none	*Eumerus armatus* Ricarte & Rotheray, 2012	*E.tricolor*	none	M	Greece, Samos, near Platanos, 37.740527, 26.742116, 09/06/2010
EU276	FSUNS:08910	**KY865507**	KY272852	none	*Eumerus pannonicus* Ricarte, Vujić & Radenković, 2016	*E.strigatus*	none	F	Serbia, Mokrin, Pašnjacivelikedroplje, 45.90615, 20.3018, 11/06/2014
EU297	FSUNS:06366	**KY865508**	KX083386	none	*Eumerus minotaurus* Claussen & Lucas, 1988	*E. minotaurus*	*E. minotaurus*	F	Greece, Lassithi, Iraklion, 7 km prePlateau of Lassithi, 35.211883, 25.461649, 22/04/2014
EU298	FSUNS:06452	**KY865509**	**KY865457**	none	*Eumerus minotaurus* Claussen & Lucas, 1988	*E. minotaurus*	*E. minotaurus*	M	Greece, Chania, 3 km pre Armeni, 35.285761, 24.468983, 25/04/2014
EU300	FSUNS:06557	**KY865510**	**KY865458**	**KY865549**	*Eumerus karyates* Chroni, Grković & Vujić, sp. n.	*E. minotaurus*	*E. minotaurus*	M	Greece, Peloponnese, Karyes, 25km N from Sparti, 37.304145, 22.421241
EU302	FSUNS:06710	**KY865511**	**KY865459**	none	*Eumerus minotaurus* Claussen & Lucas, 1988	*E. minotaurus*	*E. minotaurus*	F	Greece, Chania, Imbors, 35.252332, 24.174351, 27/05/2014
EU303	FSUNS:06728	**KY865512**	**KY865460**	**KY865547**	*Eumerus minotaurus* Claussen & Lucas, 1988	*E. minotaurus*	*E. minotaurus*	M	Greece, Chania, Omalos plain, 35.322592, 23.930496, 28/05/2014
EU320	FSUNS:06561	**KY865513**	KX083382	none	*Eumerus sogdianus* Stackelberg, 1952	*E. strigatus*	none	F	Greece, Peloponnese, Karyes2, 25km N from Sparti, 37.30416, 22.42106
EU37	FSUNS:G2286	**KY865495**	**KY865447**	none	*Eumerus crassus* Grković, Vujić & Radenković, 2015	*E. minotaurus*	none	M	Greece, Lesvos, Argennos, 39.357622, 26.254769, 03-04/06/2012
EU406	FSUNS:E1333	**KY865514**	**KY865461**	none	*Eumerus sulcitibius* Róndani, 1868	*E. sulcitibius*	none	F	Greece, Lassithi, Psichro, 35.15, 25.4666667, Unknown

Table 1 continued

Sequence ID	Specimen voucher	3'-end fragment of COI	5'-end fragment of COI	28S	Species name	Species group	Species subgroup	Sex	Field data
EU459	FSUNS:E1260	**KY865515**	**KY865462**	none	*Eumerus amoenus* Loew, 1848	*E. strigatus*	none	F	Greece, Mt Taygetos, Lok I, 37.066156, 22.265413, 06/08/2014
EU469	FSUNS:07982	**KY865516**	KX083351	none	*Eumerus clavatus* Becker, 1923	*E. clavatus*	none	F	Turkey, Mt Davraz, ski center, 37.781694, 30.75871
EU499	FSUNS:GO290	**KY865517**	**KY865463**	none	*Eumerus crassus* Grković, Vujić & Radenković, 2015	*E. minotaurus*	none	F	Greece, Samos, Neochori, 37.707965, 26.769917, Unknown
EU73	FSUNS:G0292	**KY865496**	KX083373	none	*Eumerus consimilis* Šimić &Vujić, 1996	*E. strigatus*	none	M	Serbia, Djerdap, 44.54104, 22.02024, 01/09/2011
EU75	FSUNS:G0992	**KY865497**	**KY865448**	none	*Eumerus clavatus* Becker, 1923	*E. basalis*	none	M	Greece, Ikaria, near Hristos, 37.601523, 26.084755, 11/06/2010
EU99	FSUNS:G2219	**KY865498**	**KY865449**	none	*Eumerus ornatus* Meigen, 1822	*E. ornatus*	none	M	Montenegro, Boka Kotorska, Morinj Bay, 42.490394, 18.648914, 08/10/2010
GUN5	FSUNS:GUN5	**KY865492**	KX083393	**KY865574**	*Megatrigon tabanoides* Doczkal, Radenković, Lyneborg & Pape, 2015	Outgroup	none	M	South Africa, Unknown
Y1711E	MZH:Y1711	**KY865491**	**KY865444**	*KM224496 (GB)*	*Platynochaetus setosus* Fabricius, 1794	Outgroup	none	M	France, Banyuls-sur-Mer, Pyrenées-Orientales, JardinMediterranéen, 42.474144, 3.117728
EU558	MAegean:UOTA_MEL082471, 10064	**KY865518**	**KY865464**	none	*Eumerus pulchellus* Loew, 1848	*E. pulchellus*	none	M	Greece, Anafi, Helicodrome, 36.3565, 25.7736, 15-17/06/2013
TS240	FSUNS:06666	**KY865520**	**KY865466**	**KY865552**	*Eumerus minotaurus* Claussen & Lucas, 1988	*E. minotaurus*	*E. minotaurus*	M	Greece, Rethymnon, Fotinos, 35.285762, 24.468983, 26/05/2014
TS241	FSUNS:6724	**KY865521**	**KY865467**	none	*Eumerus minotaurus* Claussen & Lucas, 1988	*E. minotaurus*	*E. minotaurus*	F	Greece, Chania, Omalos plain, 35.322592, 23.930496, 28/05/2014
MN1	FSUNS:11413	**KY865522**	**KY865468**	**KY865558**	*Eumerus phaeacus* Chroni, Grković & Vujić, sp. n.	*E. minotaurus*	*E. minotaurus*	M	Greece, Corfu, nr Ano Korakiana, 39.69882, 19.786956, 24/05/2016
MN2	FSUNS:11415	**KY865523**	**KY865469**	**KY865572**	*Eumerus phaeacus* Chroni, Grković & Vujić, sp. n.	*E. minotaurus*	*E. minotaurus*	M	Greece, Corfu, nr Ano Korakiana, 39.69882, 19.786956, 24/05/2016
MN3	FSUNS:11419	**KY865524**	**KY865470**	**KY865565**	*Eumerus phaeacus* Chroni, Grković & Vujić, sp. n.	*E. minotaurus*	*E. minotaurus*	M	Greece, Corfu, nr Ano Korakiana, 39.69882, 19.786956, 24/05/2016
MN4	FSUNS:11458	**KY865525**	**KY865471**	**KY865566**	*Eumerus phaeacus* Chroni, Grković & Vujić, sp. n.	*E. minotaurus*	*E. minotaurus*	M	Greece, Corfu, nr Liapades, 39.673537, 19.756369, 24/05/2016
MN5	FSUNS:11457	**KY865526**	**KY865472**	**KY865570**	*Eumerus phaeacus* Chroni, Grković & Vujić, sp. n.	*E. minotaurus*	*E. minotaurus*	M	Greece, Corfu, nr Liapades, 39.673537, 19.756369, 24/05/2016
MN6	FSUNS:11546	**KY865527**	**KY865473**	**KY865569**	*Eumerus phaeacus* Chroni, Grković & Vujić, sp. n.	*E. minotaurus*	*E. minotaurus*	M	Greece, Corfu, nr Strinilas, 39.739862, 19.837306, 24/05/2016
MN7	FSUNS:11461	**KY865528**	**KY865474**	**KY865555**	*Eumerus phaeacus* Chroni, Grković & Vujić, sp. n.	*E. minotaurus*	*E. minotaurus*	F	Greece, Corfu, nr Liapades, 39.673537, 19.756369, 24/05/2016
MN8	FSUNS:11460	**KY865529**	**KY865475**	**KY865548**	*Eumerus phaeacus* Chroni, Grković & Vujić, sp. n.	*E. minotaurus*	*E. minotaurus*	M	Greece, Corfu, nr Liapades, 39.673537, 19.756369, 24/05/2016
MN9	FSUNS:11448	**KY865530**	**KY865476**	**KY865551**	*Eumerus phaeacus* Chroni, Grković & Vujić, sp. n.	*E. minotaurus*	*E. minotaurus*	M	Greece, Corfu, nr AnoKorakiana, 39.69882, 19.786956, 24/05/2016
MN10	FSUNS:11430	**KY865531**	**KY865477**	**KY865559**	*Eumerus phaeacus* Chroni, Grković & Vujić, sp. n.	*E. minotaurus*	*E. minotaurus*	M	Greece, Corfu, nr Ano Korakiana, 39.69882, 19.786956, 24/05/2016
MN11	FSUNS:11459	**KY865532**	**KY865478**	**KY865561**	*Eumerus phaeacus* Chroni, Grković & Vujić, sp. n.	*E. minotaurus*	*E. minotaurus*	M	Greece, Corfu, nr Liapades, 39.673537, 19.756369, 24/05/2016

Table 1 continued

Sequence ID	Specimen voucher	3'-end fragment of COI	5'-end fragment of COI	28S	Species name	Species group	Species subgroup	Sex	Field data
MN12	FSUNS:11432	**KY865533**	**KY865479**	**KY86555**	*Eumerus phaeacus* Chroni, Grković & Vujić, sp. n.	*E. minotaurus*	*E. minotaurus*	M	Greece, Corfu, nr Ano Korakiana, 39.69882, 19.786956, 24/05/2016
MN13	FSUNS:11436	**KY865534**	**KY865480**	**KY865567**	*Eumerus phaeacus* Chroni, Grković & Vujić, sp. n.	*E. minotaurus*	*E. minotaurus*	M	Greece, Corfu, nr Ano Korakiana, 39.69882, 19.786956, 24/05/2016
MN14	FSUNS:11426	**KY865535**	**KY865481**	**KY865562**	*Eumerus phaeacus* Chroni, Grković & Vujić, sp. n.	*E. minotaurus*	*E. minotaurus*	M	Greece, Corfu, nr Ano Korakiana, 39.69882, 19.786956, 24/05/2016
MN15	FSUNS:11437	**KY865536**	**KY865482**	**KY865560**	*Eumerus phaeacus* Chroni, Grković & Vujić, sp. n.	*E. minotaurus*	*E. minotaurus*	M	Greece, Corfu, nr Ano Korakiana, 39.69882, 19.786956, 24/05/2016
MN16	FSUNS:11310	**KY865537**	**KY865483**	**KY865573**	*Eumerus crassus* Grković, Vujić & Radenković, 2015	*E. minotaurus*	none	F	Greece, Lesvos, Neochori I, 39.024073, 26.321613, 03/5/2016
MN18	FSUNS:11411	**KY865538**	**KY865484**	**KY865556**	*Eumerus karyates* Chroni, Grković & Vujić, sp. n.	*E. minotaurus*	*E. minotaurus*	M	Greece, Peloponnese, Karyes, 25km N from Sparti, 37.304145, 22.421241
MN19	FSUNS:11412	**KY865540**	**KY865485**	**KY865564**	*Eumerus karyates* Chroni, Grković & Vujić, sp. n.	*E. minotaurus*	*E. minotaurus*	F	Greece, Peloponnese, Karyes, 25km N from Sparti 37.304145, 22.421241
MN20	FSUNS:11572	**KY865539**	**KY865486**	**KY865554**	*Eumerus karyates* Chroni, Grković & Vujić, sp. n.	*E. minotaurus*	*E. minotaurus*	F	Greece, Peloponnese, Karyes, 25km N from Sparti, 37.304145, 22.421241
MN21	FSUNS:11573	**KY865541**	**KY865487**	**KY865557**	*Eumerus karyates* Chroni, Grković & Vujić, sp. n.	*E. minotaurus*	*E. minotaurus*	F	Greece, Peloponnese, Karyes, 25km N from Sparti, 37.304145, 22.421241
MN22	FSUNS:11574	**KY865542**	**KY865488**	**KY865563**	*Eumerus karyates* Chroni, Grković & Vujić, sp. n.	*E. minotaurus*	*E. minotaurus*	F	Greece, Peloponnese, Karyes, 25km N from Sparti, 37.304145, 22.421241
MN23	FSUNS:11571	**KY865543**	**KY865489**	**KY865571**	*Eumerus karyates* Chroni, Grković & Vujić, sp. n.	*E. minotaurus*	*E. minotaurus*	M	Greece, Peloponnese, Karyes, 25km N from Sparti, 37.304145, 22.421241
MN24	FSUNS:11410	**KY865544**	**KY865490**	**KY865568**	*Eumerus karyates* Chroni, Grković & Vujić, sp. n.	*E. minotaurus*	*E. minotaurus*	F	Greece, Peloponnese, Karyes, 25km N from Sparti, 37.304145, 22.421241
TS24	FSUNS:08451	*LN890909 (GB)*	**KY865445**	**KY865575**	*Merodon erivanicus* Paramonov, 1925	Outgroup	none	M	Turkey, Isparta, Geledost, Yesilkoy, 42.250833, 32.351111, 29/05/2014

Museum of Amsterdam (The Netherlands, ZMAN) and one Austrian representative of *E. longicornis* (deposited in FSUNS, which possesses two labels: "longicornis det. Schiner" and "Austria Alte Sammlung"). Outgroup taxa used in the phylogenetic analyses consisted of *Platynochaetus setosus* Fabricius, 1794 (Accession Nos. KY865491, KY865444, KM224496), *Merodon erivanicus* Paramonov, 1925 (Accession Nos. LN890909, KY865445, KY865575) and *Megatrigon tabanoides* Johnson, 1898 (Accession Nos. KY865492, KX083393, KY865574). Two sequences used for *P. setosus* (28S) and *M. tabanoides* (COI) were retrieved from GenBank. More details regarding the locality information and GenBank accession numbers for the specimens employed in the molecular analyses are enlisted in the Appendix.

Morphological characters used in the descriptions and drawings are based on the terminology established by Thompson (1999), and those related to male genitalia follow Doczkal (1996) and Hurkmans (1993). Colour characters are described from dry-mounted specimens. Male genitalia were extracted from specimens using standard methods described in Grković *et al*. (2015). Figures and drawings were generated from photographs of characters taken with a Leica DFC 320 (Wetzlar, Germany) camera attached to a Leica MZ16 binocular stereomicroscope and then processed in Adobe Photoshop CS3 v10.0 (Adobe Systems, San Jose, CA, USA). An ocular micrometer attached to a stereomicroscope was used for measurements. All measurements for a given view were conducted in the same plane. The width of the

face and head were measured in line with the lower margin of the antennal sockets, in frontal view. The proportions of the antennal segments were measured from the outside. We defined the width of the vertex as the distance between the eyes at the posterior margins of the posterior ocelli. The length of the frons was measured from the eyes to the upper margin of the antennal socket. The widths of tergites 3 and 4 were measured in line with their anterior margin and the width of the abdomen across widest part. The lengths of the tergites and abdomen were measured along a median line. Abbreviations used in descriptions are: T - tergite, S - sternite, IL - interior accessory lobe of posterior surstyle lobe.

Molecular analyses

DNA amplification and sequencing

Genomic DNA extractions were performed on two to three legs from each specimen, based on the protocol of Chen *et al*. (2010) with slight modifications as described in Grković *et al*. (2015). We amplified (a) 3' and 5' fragments of mitochondrial gene Cytochrome c oxidase subunit I (COI), and (b) nuclear gene 28S ribosomal DNA (28S D2 rDNA: covering the D2 variable region, also referred to as the second expansion region or second divergent domain). The 28S marker was amplified for 29 out of the 52 specimens. The primers used for the PCR amplification and sequencing are listed in Table 2. PCR amplifications and purification of the PCR products were performed as described in Grković *et al*. (2015). DNA sequencing was conducted based on the Sanger method on an ABI 3730 DNA analyzer (Applied Biosystems, USA) at the Sequencing Service laboratory of the Finnish Institute for Molecular Medicine (http://www.fimm.fi) and by Macrogen Inc. (The Netherlands; http://www.macrogen.com/eng/).

Sequence analysis

Raw sequences were examined and proofread in BioEdit v7.2.5 (Hall, 1999). Multiple sequence alignments were implemented in MAFFT v7 by

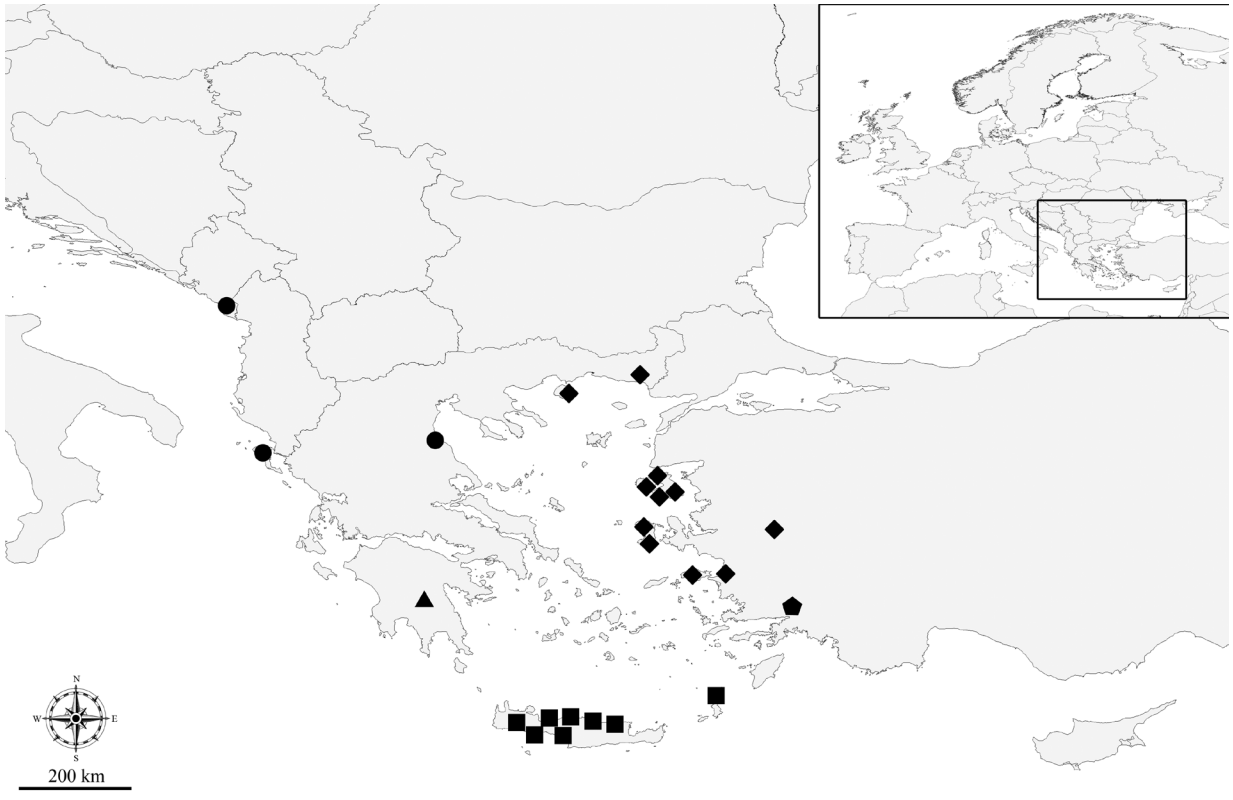

Figure 2. Distributions of all specimens used for the morphological, molecular and wing morphometric analyses. ■ *E. minotaurus*, ▲ *E. karyates* sp. n., ● *E. phaeacus* sp. n., ◆ *E. crassus*, ⬟ *E. anatolicus* sp. n.

Table 2. Primers used for amplification and sequencing of the mtDNA and nDNA gene fragments.

	Primer pair	Primer sequence	Source
3' fragment of COI	C1-J-2183 (alias Jerry)	5'-CAACATTTATTTTGATTTTTTGG-3'	Simon et al., 1994
	TL2-N-3014 (alias Pat)	5'-TCCAATGCACTAATCTGCCATATTA-3'	Simon et al., 1994
5' fragment of COI	LCO-1490	5'-GGTCAACAAATCATAAAGATATTG-3'	Folmer et al., 1994
	HCO-2198	5'-TAAACTTCAGGGTGACCAAAAAATCA-3'	Folmer et al., 1994
28s D2 rDNA	28S (F2)	5'-AGAGAGAGTTCAAGAGTACGTG-3'	Belshaw et al., 1998
	28S (3DR)	5'-TAGTTCACCATCTITCGGGTC-3'	Belshaw et al., 1998

employing the L-INS-i algorithm (see supplementary information, Data S1, S2; Katoh *et al*., 2005; available at http://mafft.cbrc.jp/alignment/server/index.html). Polymorphic sites, parsimony informative sites and number of haplotypes were calculated using DnaSP v5.10.01 (Librado and Rozas, 2009).

Phylogenetic analyses and tree-based species delimitation

We constructed three datasets to elucidate and corroborate the phylogenetic positions of four species within the *E. minotaurus* group (*E. anatolicus* sp. n. was excluded due to unavailability of DNA sequences) : (1) COI dataset, based on a concatenation of the 3' and 5' fragments of the COI gene (19 *Eumerus* taxa, 1238 bp); (2) 28S dataset, based on the 28S nuclear gene fragment (4 *Eumerus* taxa, 510 bp); and (3) COI subset, based on a concatenation of the 3' and 5' fragments of the COI gene for the *E. minotaurus* group alone (4 *Eumerus* taxa, 1238 bp) (for more details, see Table3). Representatives of other species of *Eumerus* (15 species) were only considered for the COI dataset in order to properly display phylogenetic positions and relationships of the species encompassing the *E. minotaurus* group. The phylogenetic positions and species delimitation of these 15 species were previously confirmed and discussed in Chroni *et al*. (2017) and Grković *et al*. (2017), thus we argue that the singletons used here do not jeopardize our phylogenetic inferences. The distinct morphologies of these 15 species were also accounted in species delimitation, and confirmed by the taxonomists Ante Vujić and Ana Grković.

We have inferred various phylogenetic analyses for the COI dataset as to clarify and corroborate the species topology: Maximum parsimony (MP), Maximum likelihood (ML), Neighbour joining (NJ), Bayesian inference (BI) and split network analyses. MP analyses were performed in NONA (Goloboff, 1999), spawned in WINCLADA v1.00.08 (Nixon, 2002). A heuristics search algorithm with 1000 random addition replicates (mult x 1000) was performed with holding of 100 trees per round (hold / 100), max trees set to 100 000, and applying TBR branch swapping. The ML analysis was executed in RAxML v8.0.9 (Stamatakis, 2006; Stamatakis *et al*., 2008) in the Cipres Science Gateway (Miller *et al*., 2010) with 1000 bootstrap replicates. The ML analysis was implemented under the general time-reversible (GTR) evolutionary model with a gamma distribution (GTR+G; Rodriguez *et al*., 1990) since it is the most accurate substitution model for datasets of approximately 50 taxa. We sought the best-fit substitution model for the COI dataset in MEGA v6.06 (Tamura *et al*., 2013), resulting in identification of the GTR+G+I model, as proposed by the Bayesian Information Criterion (BIC). We employed MEGA v6.06 (Tamura *et al*., 2013) to perform NJ analyses, but used the Tamura-Nei (TN93) nucleotide substitution model with a Gamma distribution (*i.e*. the second-best nucleotide substitution model proposed by BIC) since GTR model is not allowable in MEGA for NJ trees, and using 1000 bootstrap replicates. We assessed BI tree in MrBayes v3.2.6 (Huelsenbeck and Ronquist, 2001) in the Cipres Science Gateway (Miller *et al*., 2010) under the GTR+G+I model, as proposed by the BIC (Rodriguez *et al*., 1990). We partitioned our sequence data by codon (two partitions; positions 1st+2nd; 3rd), which as it is recommended for protein-encoding genes as the third codon position is considered to be susceptible to higher mutational rates

(Shapiro *et al*., 2006; Simmons *et al*., 2006; Bofkin and Goldman, 2007). The settings for the Bayesian Markov chain Monte Carlo (MCMC) process included two runs of $10*10e^{-6}$ MCMC generations (×4 chains) with a sampling frequency of 1000 generations and a relative burn-in of 10%. MCMC results were checked with TRACER v1.6 (http://tree.bio.ed.ac.uk/software/tracer/; Rambaut *et al*., 2014) and the tree was displayed in FigTree v1.4.2 (http://tree.bio.ed.ac.uk/software/figtree/; Rambaut, 2013). ML, NJ and BI trees were merged into a split network in order to extract a united tree topology. The split network was produced in SplitsTree4 v4.14.3 (Huson and Bryant, 2006) (http://www.splitstree.org/) under the parameters SuperTree, Z-closure super-network from partial trees, and heuristic analysis (number of runs: 1000). Regarding the 28S dataset, we employed MP analysis, as described above. All phylogenetic trees were rooted on *P. setosus*.

In addition, Poisson tree processes (PTP) models were implemented in order to highlight putative molecular species clusters (Zhang *et al*., 2013) based on the best ML tree resulting from the RA×ML analysis of the COI dataset. PTP analyses were conducted on the web server for PTP (available at http://species.h-its.org/ptp/).

Non-tree-based species delimitation

As to compare and confirm the indication of the *E. minotaurus* complex, non-tree-based species delimitation approaches were performed as well. Average pairwise Kimura 2-parameter (K2P) distances between the taxa of the COI dataset, and overall sequence divergence (under the TN93+G+I model for the COI dataset and the COI subset, and under the Tamura 3-parameter for the 28S dataset; Tamura *et al*., 2013) were estimated in MEGA v6.06 (Tamura *et al*., 2013) and proposed by BIC. We have considered a threshold of2% sequence divergence (the barcode gap) for species delimitation (outgroups were excluded; Ratnasingham and Hebert, 2013).

Network approaches can be more effective than classical phylogenetic ones for representing intraspecific evolution (Posada and Crandall, 2001), so we assessed genealogical relationships between haplotypes of the COI subset with haplotype networks constructed using the statistical parsimony algorithm implemented in the program TCS v1.21 (Clement *et al*., 2000) under the 95% connection limit of parsimony (gaps treated as missing data).

Molecular divergence time estimates

We created the COI subset to estimate a time-calibrated species tree, and to reconstruct the biogeographic history of species encompassing the *E. minotaurus* group, *i.e. E. crassus*, *E. karyates* sp. n., *E. minotaurus* and *E. phaeacus* sp. n.

Initially, we explored temporal structure in the COI subset –necessary prerequisite for reliable estimation of substitution rates– by performing a regression of root-to-tip genetic distances in TempEst (Rambaut *et al*., 2016). We used the NJ tree (generated for the COI subset as described above) as the input file.

Subsequently, we estimated divergence times using BEAST v1.8.4 (Drummond *et al*., 2012). The input file (.xml) was created using BEAUti v1.8.4, and we integrated the BEAGLE library (Ayres *et al*., 2012) into BEAST runs to achieve high-performance computing. Applied prior specifications were as follows: Relaxed Uncorrelated Lognormal Clock; Birth Death process of speciation; TN93 model with G rate heterogeneity. We also partitioned the dataset by codon (two partitions: positions 1st+2nd; 3rd, Shapiro *et al*., 2006; Simmons *et al*., 2006; Bofkin and Goldman, 2007). We have considered three approaches to calibrate the molecular clock, with employment of: (a) one calibration point based on the MAT event that separated the Aegean archipelago into its western and eastern parts (10.5 ± 1.5 My, MAT analysis, Papadopoulou *et al*., 2010); (b) two calibration points where the root height was based on the MAT event and the prior of the taxon subset *E. karyates* sp. n./*E. minotaurus* was based on the end of the MSC event that represents permanent isolation of Crete from the Greek mainland (5.3 ± 0.3 My, MAT&MSC analysis, Kasapidis *et al*., 2005; Kamilari *et al*., 2014); and (c) 2.3% pairwise evolutionary rate per million years (My), representing the standard arthropod substitution rate for mtDNA (mtDNA-rate analysis, Brower, 1994). We also created: (i) four taxon subsets based on estimates for each of the four species within the *E. minotaurus* group for the MAT and mtDNA-rate analyses; and (ii) two taxon subsets, one with *E. crassus* sequences and one with sequences of *E. karyates* sp. n./*E. minotaurus* for the MAT&MSC analysis in order to log the time to the most common ancestor tMRCA for each taxon subset and to set the prior distributions for corresponding divergence times. Three independent runs were performed with a chain length of $10*10e^{-6}$ iterations for the MAT and MAT&MSC analyses and $5*10e^{-6}$ iterations for the mtDNA-rate analysis, sampled every 1000 generations. The program TRACER v1.6

(http://tree.bio.ed.ac.uk/software/tracer/; Rambaut *et al*., 2014) was employed to confirm stationarity. Independent runs were combined using Logcombiner v1.8.4 (in BEAST). The final tree with divergence time estimates was summarized with TreeAnnotator v1.8.4 (in BEAST; 10% of trees were discarded as burn-in; Maximum clade credibility tree; and Mean heights) and visualized with FigTree v1.4.2 (http://tree.bio.ed.ac.uk/software/figtree/; Rambaut, 2013).

Biogeographic analyses

To reconstruct the biogeographic history and to predict biogeographic ancestral ranges of the *E. minotaurus* group (COI subset), we conducted the statistical approach of Bayesian Binary MCMC (BBM) Method For Ancestral State (Ronquist and Huelsenbeck, 2003), conducted in RASP v3.2 (Yu *et al*., 2015). The MCMC chains were run by default, and the annotated trees from the BEAST analyses were used as input tree files. Four geographical areas were defined based on the clustering and distribution of the *E. minotaurus* group lineages as well as on (recorded) plant distributions (Brummitt *et al*., 2001; Strid, 2016): (A) Crete and Karpathos, (B) Peloponnese, (C) Balkan Peninsula, and (D) East Aegean islands (Appendix). Ancestral ranges were assumed to include from one to four areas.

Geometric morphometric analysis

Geometric morphometric analysis of wing shape was conducted on 51 specimens of the *E. minotaurus* group (see supplementary information S1). The right wing of each specimen was removed by means of a micro-scissors and was then mounted in Hoyer's medium on a microscopic slide. Wings have been archived and labelled with a unique code in the FSUNS collection, together with other data relevant to the specimens. High-resolution photographs of the wings were made using a Leica DFC320 video camera attached to a Leica MZ16 stereomicroscope. Ten homologous landmarks at vein intersections or terminations (that could be reliably identified) were selected using TpsDig v2.05 (Rohlf, 2006). Each wing was digitized three times to estimate the measurement error, and average landmark coordinates for each individual were used in analyses (Arnqvist and Mårtensson, 1998). All geometric morphometric analyses were conducted on a dataset in which both sexes were pooled and the male dataset separately, with allometry corrected for both datasets.

Generalised least squares Procrustes superimposition was performed in MorphoJ v2.0 (Klingenberg, 2011) on the raw coordinates to minimize non-shape variations in location, scale and orientation of

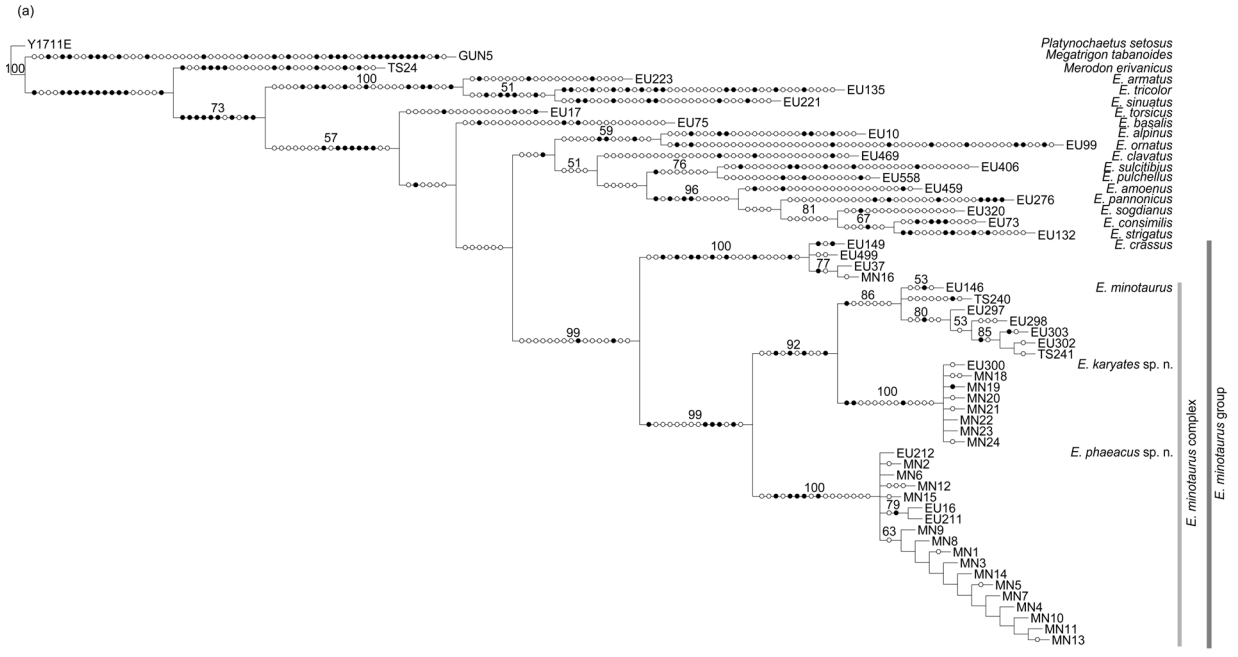

Figure 3. Maximum parsimony analyses for the concatenated 3' and 5' fragments of the COI gene (COI dataset). Only the condensed tree is illustrated here. Filled circles denote unique changes and open circles non-unique changes. Bootstrap support values are illustrated above the branches: 60 trees, Length 1122 steps, CI=44, RI=72.

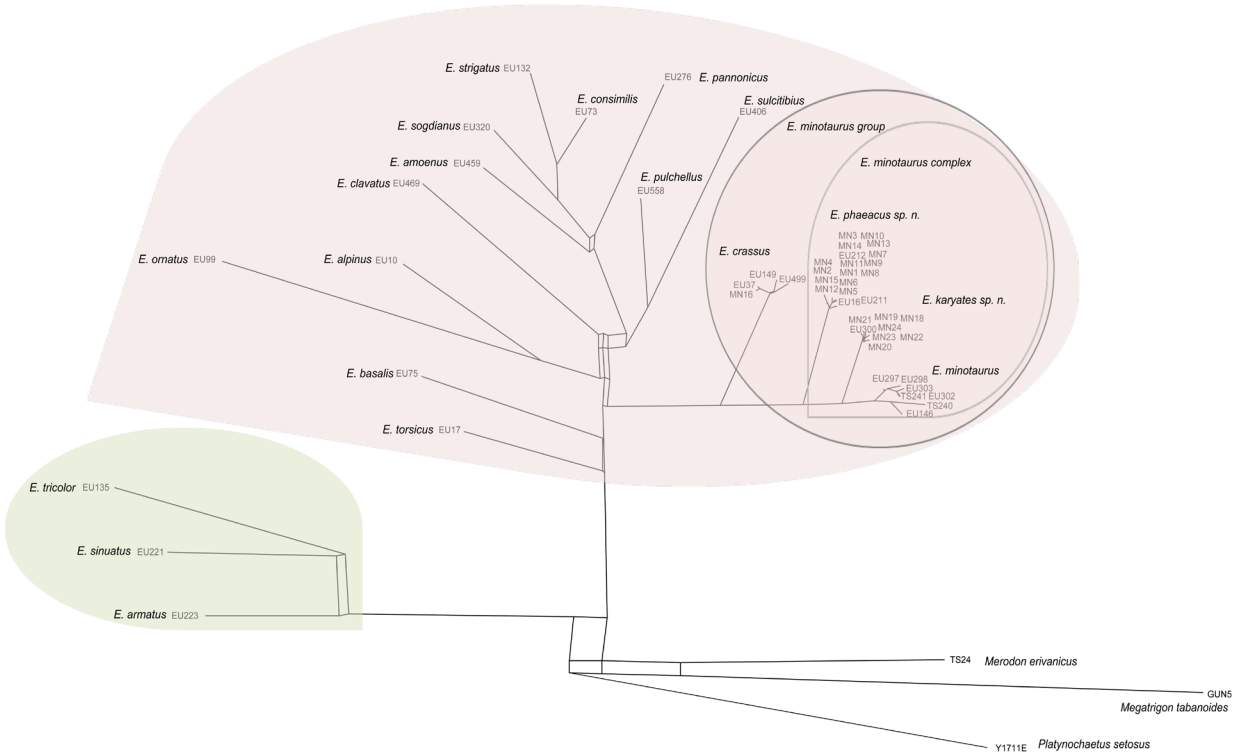

Figure 4. A phylogenetic network of ML, NJ and BI tree results for the concatenated 3' and 5' fragments of the COI gene (COI dataset).

wings, and to superimpose the wings in a common coordinate system (Rohlf and Slice, 1990; Zelditch *et al*., 2004). Principal component analysis was carried out on the Procrustes shape variables to reduce the dimensionality of the data set. All further statistical analyses were conducted in the reduced space using a subset of independent principal components (PCs) that describe the highest overall classification percentage calculated in stepwise discriminant analysis (Baylaac and Frieß, 2005).

To explore wing shape variation among the taxa, we employed canonical variate (CVA) and discriminant function analysis. Additionally, a Gaussian naïve Bayes classifier was used to delimit species boundaries based on wing shape variation without *a priori*-defined groups. Phenetic relationships among taxa were determined by UPGMA analysis based on squared Mahalanobis distances computed from the discriminant function analysis applied to wing shape variables. Superimposed outline drawings produced in MorphoJ v2.0 (Klingenberg, 2011) were used to visualize differences in mean wing shape among species pairs. All statistical analyses were performed in Statistica for Windows (Dell Statistica, 2015).

Correlation among wing shape, genetic, spatial and climatic differentiation

To test correlations between morphometric, genetic, geographic and climatic distances among species, we performed Mantel tests (Mantel, 1967) with 10 000 permutations in PaSSaGe (Rosenberg and Anderson, 2011). Morphometric distances were represented as a matrix of pairwise squared Mahalanobis distances, and genetic distances as a matrix of uncorrected p distances (as calculated in MEGA v6.06; Tamura *et al*., 2013). Geographic distances were calculated as the minimum distance between two species using QGIS (Quantum GIS Development Team, 2012). Climatic distances were represented as Euclidean distances of the factor scores calculated based on 19 bioclimatic variables generated for each locality from the current climate WorldClim dataset (2.5 arc-minutes resolution) (Hijmans *et al*., 2005).

Two-tailed Mantel tests were performed to test pairwise correlations among the four distance matrices, and partial Mantel tests were used to explore relationships between: (i) wing shape and genetic differentiation, while accounting for the

Table 3. Characteristics for each analyzed dataset; in the 'Sequences no' the number of outgroups is not considered.

Dataset	COI	28S	subset COI
Gene fragment(s)	3' and 5' fragment of COI	28s D2 rDNA	3' and 5' fragment of COI
Taxa no	19	4	4
Sequences no	52	29	37
Sequence length (bp)	1238	510	1238
Singleton variable sites	86	11	18
Parsimony informative sites	258	2	100
Sequence divergence (%)	6.1	0.3	2.8
Haplotypes no (with gaps/missing data: not considered)	41	3	26
Geographical clusters no (BBM analysis)	-	-	4

effect of geographic distances and climatic distances separately; and (ii) wing shape and geographic distances accounting for the genetic distances.

Results

Molecular analyses

Phylogenetic analyses: tree-based and non-tree-based species delimitation

All tree-based (MP, ML, NJ, BI, split network and PTP models, high bootstrap and probability support values; Figures 3, S2, S3, S4 and 4, respectively) and non-tree-based (K2P, TCS) species delimitation analyses of the COI dataset (1238 bp) indicated four, well-supported, clusters-species within the *E. minotaurus* group as well as three species within *E. minotaurus*, revealing the *E. minotaurus* complex. The PTP analysis returned an estimation of 22 to 26 lineages, with four within the *E. minotaurus* group. Interspecific genetic distances (K2P) for the COI dataset were found to be 0.025-0.117 (except for specimen TS241, 0.014). Sequence divergence was calculated for both the COI and 28S datasets, as well for the COI subset (Table 3). TCS analysis for the COI subset led to four independent networks, one for each species within the *E. minotaurus* group (S5).

Unlike the mitochondrial marker (COI dataset; S6), the nuclear molecular marker (28S dataset) could not distinguish evolutionary lineages. Moreover, the low sample size (4 species, 29 sequences) and the short sequence length (510 bp) meant we considered it of no benefit to further analyze the 28S dataset. Therefore, only the results of the COI dataset were sought to be used for the species delimitation within the *E. minotaurus* group.

Molecular divergence time estimates and biogeographic analyses

Our root-to-tip regression revealed relatively strong temporal structure in the COI subset, with a correlation coefficient of 0.1586 (R squared= 0.02514), allowing us to implement a molecular clock model. This analysis also indicated that the sequences EU37, EU149 (*E. crassus*) and TS240 (*E. minotaurus*) are less divergent than the rest, whereas the EU297 (*E. minotaurus*) is the most divergent. The indication of few more or less divergent sequences was not considered as the quality of those sequences was checked and confirmed.

The time-calibrated species tree and the results of the BBM analysis are both depicted in Figure 5. Due to the similar probability values and for simplicity, we only present in Figure 5 the BBM results based on the annotated tree produced from the MAT analysis. The species-tree topology is congruent with that inferred from the phylogenetic analyses. Divergence time estimates, as assessed for the MAT and MAT&MSC approaches are well-nigh consistent. According to the inferred dates, diversification of the *E. minotaurus* group dates back to the Miocene, whereas speciation within the *E. minotaurus* complex approximately dates to the MSC (Figure 5). The pairwise substitution rates obtained were 0.882% and 0.706% for the MAT and MAT&MSC analyses, respectively. Divergence times for the mtDNA-rate analysis were much lower, placing the diversification of the *E. minotaurus* group and the *E. minotaurus* complex to the Pliocene and Pleistocene, respectively. All posterior probability values per lineage exceeded 0.95 (and ranged up to 1). The substitution rates were approximately 0.80 based on codon positions 1+2, and 1.36 for codon position 3.

The BBM analyses from all annotated trees were congruent and suggested a total of six dispersal and three vicariant events shaped the current distribution of the *E. minotaurus* group, and that speciation events have occurred within areas as follow: A:6, B:7, C:17 and D:3. Dispersal events may have occurred between areas: A to B (Crete and Karpathos to Peloponnese), C to A (Balkan Peninsula to Crete and Karpathos) and D to C (East Aegean Islands to Balkan Peninsula). Three possible dispersal routes are proposed for each node; I: A→BA→B→A, II: C→CA→C→A or III: D→CD→C→D (Figure 5).

Geometric morphometric evidence

Geometric morphometric analyses of wing shape showed the same pattern for pooled sexes and for the males separately, so only results based on the pooled dataset are presented here. Measurement (digitizing) error was negligible.

Principal component analysis carried out on the Procrustes shape variables produced 16 PCs (S7). Stepwise discriminant analysis revealed that the first 13 PCs represented the highest overall classification percentage of investigated taxa. Canonical variates analysis conducted on these 13 PCs produced three highly significant axes (CV1: Wilks' Lambda = 0.0165; $\chi2 = 170.219$; $p < 0.01$; CV2: Wilks' Lambda = 0.1420; $\chi2 = 80.992$; $p < 0.01$; CV3: Wilks' Lambda = 0.4413; $\chi2 = 33.949$; $p < 0.01$). CV1 clearly separated *E. crassus* from *E. phaeacus* sp. n., though *E. minotaurus* and *E. karyates* sp. n. is related with CV2 and CV3. CV2 separated *E. minotaurus* from other under study species, while CV3 showed that *E. karyates* sp. n. differs from *E. crassus*, *E. phaeacus* sp. n. and *E. minotaurus* (Figure 6). Moreover, our discriminant function analysis showed that all species pairs differed highly significantly in wing shape ($p < 0.01$) (S8). Importantly, 96% of specimens were correctly classified into *a priori*-defined groups, demonstrating that wing shape is a reliable character for interspecific discrimination. All specimens belonging to *E. crassus* and *E. phaeacus* sp. n. were correctly classified. One specimen of *E. minotaurus* and one of *E. karyates*

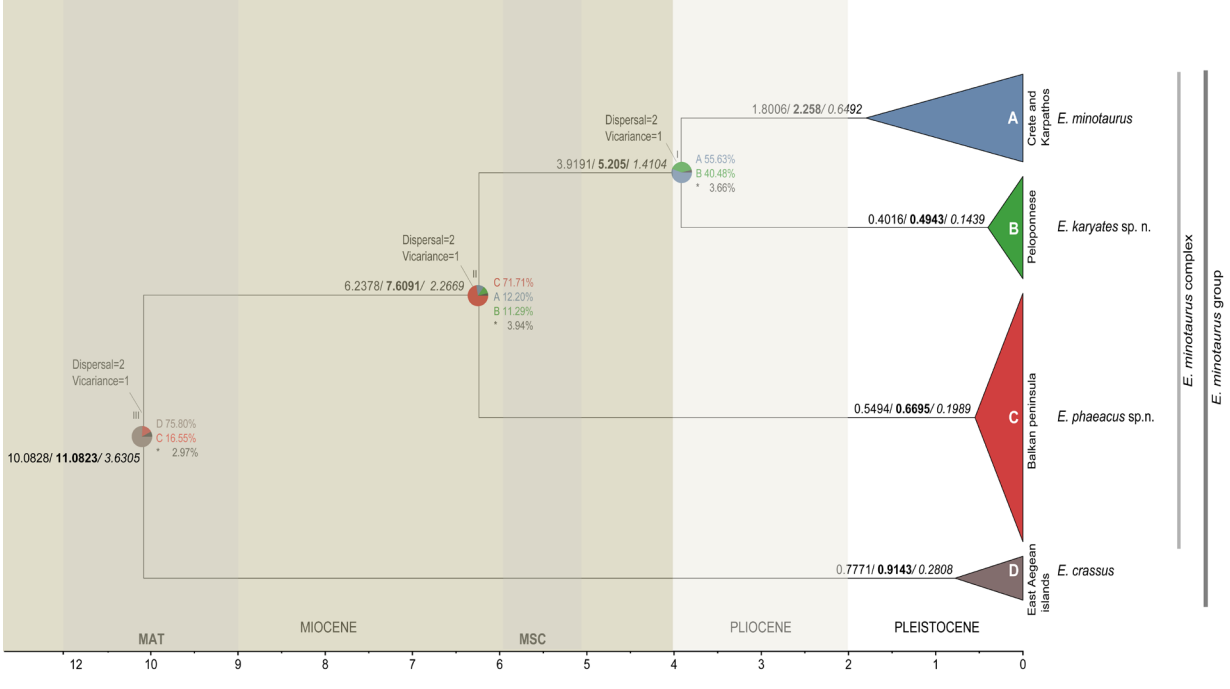

Figure 5. Trees inferred with BEAST for the concatenated 3' and 5' fragments of the COI gene (COI subset) for the *E. minotaurus* group. Values on the left and above the branches are mean ages estimated according to the uncorrelated log-normal clock based on (a) MAT (in normal text), (b) MAT&MSC (in bold), and (c) 2.3% mtDNA-rate (in italics), in Mya (a/b/c). The four defined areas are presented with different colours, percentage values (on the right side of the nodes of the tree) and pie charts at nodes I, II and III; (A) Crete and Karpathos (blue), (B) Peloponnese (green), (C) Balkan Peninsula (red), (D) East Aegean Islands (grey), and (*) unknown (black) (for interpretation of the references to colour in this figure legend, the reader is asked to refer to the web version of this article).

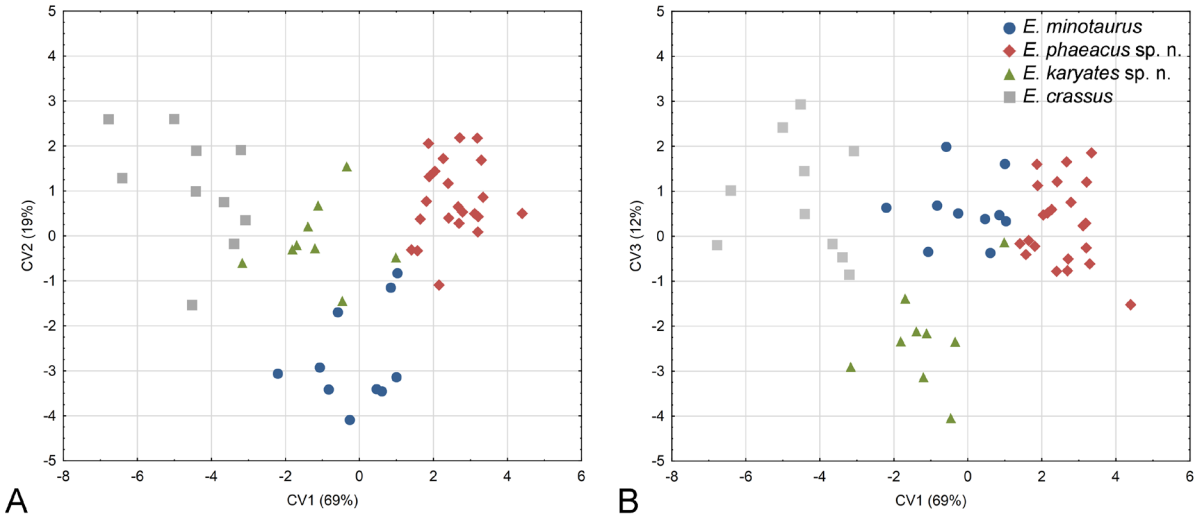

Figure 6. Shape variability among species of the *Eumerus minotaurus* species group: A) Scatter plot of individual scores of CV1 and CV2; and B) scatter plot of individual scores of CV1 and CV3.

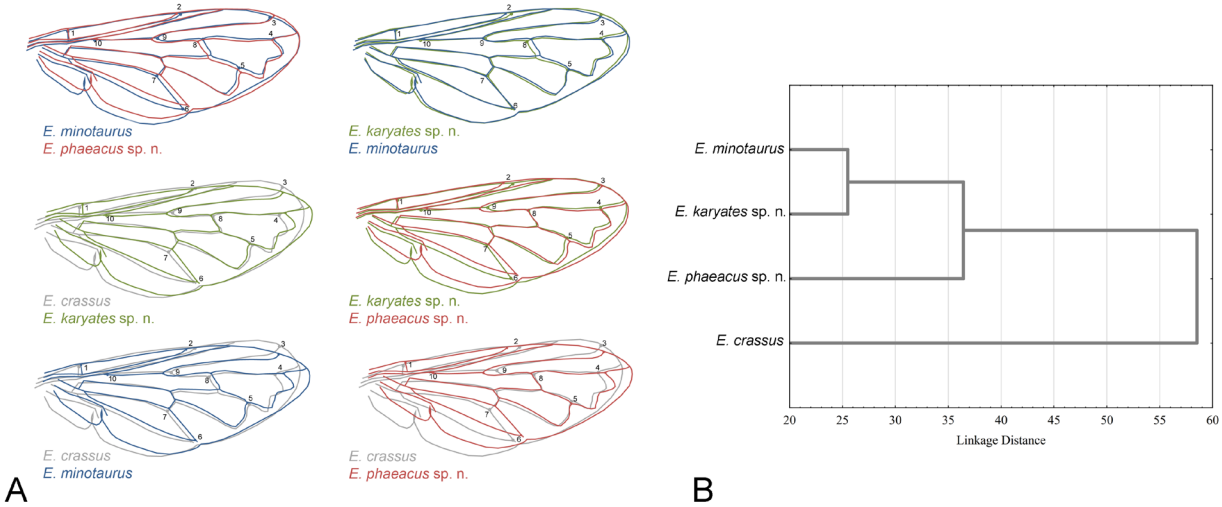

Figure 7. Wing shape differences among species of the *Eumerus minotaurus* group. A) Superimposed outline drawings showing differences in average wing shape for each species pair. Differences between the species were exaggerated three-fold to make them more visible; and B) UPGMA geo-phenogram constructed using the squared Mahalanobis distances of wing shape (for interpretation of the references to colour in this figure legend, the reader is asked to refer to the web version of this article).

Table 4. Results of simple and partial two-tailed Mantel tests for correlation among phenetic distance (wing shape) and genetic, geographic and climatic distances ($p > 0.05$).

	r
Simple Mantel test	
wing - genetic	0.75
wing - geography	0.46
wing - climate	-0.58
Partial Mantel test	
wing - genetic - holding geography	0.79
wing - genetic - holding climate	0.58
wing - geography holding genetic	-0.57

sp. n. were misclassified as *E. phaeacus* sp. n. A congruent classification was obtained by the Gaussian naive Bayes classifier, through which all specimens of *E. minotaurus*, *E. crassus* and *E. phaeacus* sp. n. were correctly classified, and only one specimen of *E. karyates* sp. n. was misclassified as *E. minotaurus*. The same male specimen of *E. karyates* sp. n. was misclassified by both approaches.

Superimposed outline drawings depict the differences in mean wing shape among each species (Figure 7A). The most obvious differences are among *E. crassus* and species of them *E. minotaurus* complex. In contrast, the most subtle differences in mean shape are between *E. minotaurus* and *E. karyates* sp. n. This is consistent with the results of our UPGMA analysis based on squared Mahalanobis distances (Figure 7B).

Correlation among wing shape, genetic, spatial and climatic differentiation

Simple Mantel tests revealed that genetic, geographic and climatic distances were not correlated with wing shape distance among *E. minotaurus*, *E. karyates* sp. n., *E. phaeacus* sp. n. or *E. crassus* (Table 4). Additionally, partial Mantel test showed that genetic distance has no impact on wing shape differentiation while accounting for geographic and environmental distances, nor did geographic while accounting for genetic distance (Table 4).

Discussion

Despite its critical role in ecosystems and the high species diversity of the genus *Eumerus*, which is continuously expanding through new species description, taxonomic issues remain. The new species within the genus (Doczkal 1996; Ricarte *et al*., 2012; Grković *et al*., 2015, 2017; Markov *et al*., 2016; van Steenis *et al*., 2017; Smit *et al*., 2017) should be incorporated into new phylogenetic and biogeographic studies. There has only been one phylogenetic study on the genus so far (Chroni *et al*., 2017), which provided genetic evidence of two major monophyletic lineages and seven 'molecular' groups within the genus *Eumerus*, including an *E. minotaurus* group.

The present study is the first to focus on the *E. minotaurus* group and, by employing an integrative framework, we reveal one new species and identify the *E. minotaurus* cryptic species complex within the genus (Figures 8, 9). Evidence for the new species is based on morphological data, and the cryptic species complex is well supported by mtDNA sequences, discrete morphological features (antennae, male genitalia), wing morphometry, and biogeographic reconstructions. We also attempted, albeit unsuccessfully, to use a nuclear marker (never previously tried before in *Eumerus*) to infer phylogenetic relationships between species of the *E. minotaurus* group. Below, we discuss our findings and further conclude with contingent biogeographic patterns and speciation processes within the *E. minotaurus* group in relation to the palaeogeography of the Aegean region.

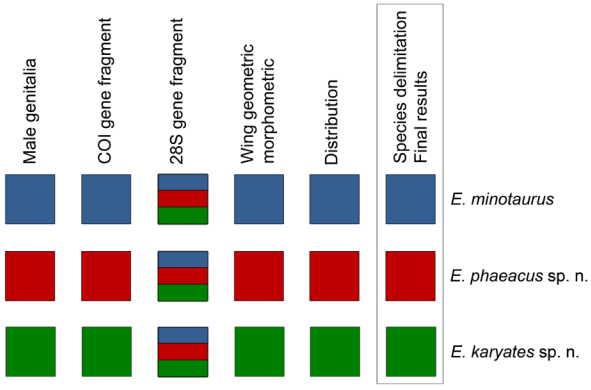

Figure 8. Summary of the results of integrative species delimitation within the *Eumerus minotaurus* complex: morphological characters (male genitalia), molecular markers (COI and 28S gene fragments), wing geometric morphometrics and geographical distribution. Each species is represented by a different colour; *E. karyates* sp. n. (green), *E. minotaurus* (blue) and *E. phaeacus* sp. n. (red). Solid colour boxes indicate successful species delimitation by particular approach. Multicolour boxes depict clusters formed by multiple species.

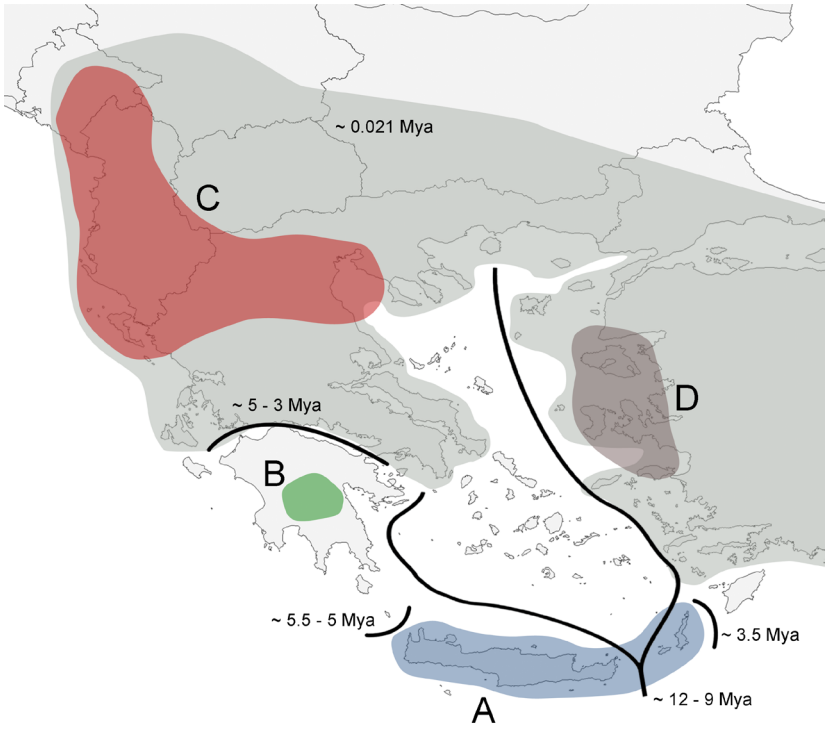

Figure 9. Mitochondrial phylogeographic pattern of the *E. minotaurus* taxon group. Specimens are grouped according to species/geographical cluster: *E. crassus*/East Aegean Islands, D; *E. karyates* sp. n./Peloponnese, B; *E. minotaurus*/Crete and Karpathos, A; and *E. phaeacus* sp. n./Balkan peninsula, C. The major geological events in the Aegean Archipelago, that led to speciation within the group are displayed, *i.e.* the formation of MAT (12-9 Mya) and separations of: Crete from the Peloponnese (5.5-5 Mya), the Peloponnese from the Greek mainland (5-3 Mya) and Karpathos from Crete (3.5 Mya). There is evidence that until the end of the Pleistocene (0.021 Mya), the Greek mainland, Anatolia and the East Aegean Islands were still linked (for interpretation of the references to colour in this figure legend, the reader is referred to the web version of this article).

Taxonomic and molecular implications

Doczkal (1996) published the first study indicating the affinity among *Eumerus* species with elongated pedicels (*i.e.* the *E. minotaurus* group) in which he described *E. niehuisi*. Taxonomic and phylogenetic analyses of *E. crassus*, *E. anatolicus* sp. n., the *E. minotaurus* complex and *E. longicornis* have evidenced their differentiation from other *Eumerus* species (Doczkal, 1996; Chroni *et al*., 2017). We argue that all these aforementioned species belong to the same taxon group (the *E. minotaurus* group) owing to all of them having an elongated pedicel and similarly shaped male genitalia, the major common features differentiating them from other *Eumerus* species and groups. Studies by Hasson *et al*. (2009) and House *et al*. (2013) indicate that natural and sexual selection (and their interaction) may promote insect genital evolution.

Our morphology-based results are supported by our mtDNA analyses. The utility of a molecular marker is determined by its ability to reveal with high resolution the phylogenetic relationships of the organism(s) being studied, which is dependent on the mutation rate of the coding region. Our mtDNA phylogenetic reconstructions (tree-based species delimitation) and putative species limits analyses (non-tree-based) reaffirmed our morphological assignments (species predictions), clustering all these species within the same phylogenetic group with quite high bootstrap and probability values, and fully supporting the configuration of the *E. minotaurus* group. In addition, the employed mtDNA sequences clearly granted three lineages representing three different species within *E. minotaurus*, proving its suitability for resolving cryptic species. Identification of these three mitochondrial lineages led us to examine the male genitalia in more detail to seek subtle differences that we consider crucial to differentiating cryptic species. Tree topologies within the *E. minotaurus* group were consistent; in all cases, the *E. crassus* lineage was distinct from that of the *E. minotaurus* complex and, within the complex, *E. karyates* sp. n. and *E. minotaurus* clustered together but apart from *E. phaeacus* sp. n.

A combination of mitochondrial and nuclear gene fragments is often preferred to discriminate evolutionary lineages; therefore we intended to incorporate a nuclear marker dataset into our phylogenetic analyses. The 28S nuclear marker has shown genetic divergence among hoverflies (Mengual *et al*., 2008), and not only (*e.g.* Awasthi *et al*., 2016). However, in our study, the 28S marker resulted in low tree resolution and lineage admixture. We detected partial (six out of

eight sequences) clustering for one species of the *E. minotaurus* complex (*E. karyates* sp. n.) in the 28S MP tree, denoting a recent speciation event, most likely not yet complete. For the remaining species of the *E. minotaurus* complex, the 28S marker proved un-informative. We had only one 28S sequence (that of *E. crassus*) outside of the *E. minotaurus* complex from which it was clearly separated, but the lack of sequences prevent us from making further conclusions about the utility of this marker for species diagnoses within *Eumerus*. We speculate that differences in lineage clustering in the trees generated by the two molecular markers are due to the faster evolutionary (mutation) rate of the mitochondrial gene fragment.

Our molecular and morphological inferences are also supported by highly significant morphological wing differentiation among species within the *E. minotaurus* complex. Although our species assignments for wing shape assessments were based on phylogenetic inferences, we consider wing shape heritability as a part of an integrative approach and a significant additive factor to our diagnosis of the cryptic species complex. Previous studies on hoverflies have shown that wing shape is a reliable predictor of interspecific differentiation, with wing geometric morphometry mainly being conducted on the genus *Merodon* (Milankov *et al*., 2009; Francuski *et al*., 2009, 2011; Ačanski *et al*., 2016; Šašić *et al*., 2016), but other examples of successful implementation of this method in hoverfly genera exist, such as in *Cheilosia* (Ludoški *et al*., 2008) and *Chrysotoxum* (Nedeljković *et al*., 2013; 2015), as well as in the hoverfly tribe Pipizini (Vujić *et al*., 2013). Moreover, in recent taxonomic studies of cryptic hoverfly species, molecular data strongly supported the results of geometric morphometrics results, even though small sample size was employed (as for the current study, Vujić *et al*., 2013; Nedeljković *et al*., 2013; 2015; Ačanski *et al*., 2016; Šašić *et al*., 2016; Radenković *et al*., 2017). This is the first study to include wing shape analyses on the genus *Eumerus* and the results are in accordance with previous hoverfly studies. Apart from the significant differences in wing shape among species, the high percentage of correct specimen assignments to species by both discriminant function analysis and the Gaussian naïve Bayes classifier analyses demonstrates that wing shape is highly reliable in cryptic species delimitation.

The topology of the phenogram based on wing shape variables was congruent with the topology inferred from phylogenetic analyses. The most similar wing shape was detected between *E. minotaurus* and *E. karyates* sp. n., and *E. crassus* wing shape was distinct from the species of the *E. minotaurus* complex. Observed differences in mean wing shape of the species within the *E. minotaurus* complex were mainly associated with broadness of the proximal part of the wing. Both proximal and distal parts of the wing differed between *E. crassus* and the *E. minotaurus* complex. Due to our small sample size, it was not possible to account for sexual dimorphism. Therefore, sexual dimorphism may bias some of our conclusions about mean wing shape differences among the investigated species. Wing length and width influence insect flight ability and male species-specific courtship song (Cowling and Burnet, 1981; Stubbs and Falk, 1983; Routtu *et al*., 2007; Sacchi and Hardersen, 2012; Menezes *et al*., 2013; Outomuro *et al*., 2013), indicating potential natural and sexual selection on wings. The Mantel tests (both simple and partial) we conducted showed no significant correlation among wing shape and current climate, or for geographic or genetic proximity. Following the statement and results mentioned above, we assume that interactions of natural selection, adaptive processes to paleogeographic conditions, phylogenetic history, and restricted gene flow of isolated ancestral populations could explain wing shape differences among the cryptic species.

Mitochondrial dating, biogeographic history and divergence time estimates

An important issue for the mitochondrial phylogeography of hoverflies (including *Eumerus*) is the absence of a fossil record and an accurate mitochondrial substitution rate for gene fragments that could be used to calibrate the molecular clock. Here, we essayed three different analytical approaches based on the two major geological events that occurred in the Aegean Archipelago (MAT and MSC) as well as the standard mitochondrial substitution rate reported for arthropods (mtDNA-rate, Brower, 1994). The mtDNA-rate is not always feasible for all insect groups, having been shown to produce unreliable results, and hence, potential pitfalls should be taken into account (Papadopoulou *et al*., 2010). Indeed, we found that the divergence times generated from our mtDNA-rate analysis were rather low and inconsistent with any major geological event of the Aegean region that could explain speciation within the *E. minotaurus* group, confirming its reputation to give ‘unrealistic ages’. In contrast, the MAT and MAT&MSC divergence

time estimates were similar, with the latter approach being more in line with biogeographic events in the region. We posit that our MAT&MSC divergence times might reflect better the actual diversification events. The low estimated pairwise substitution rates arising from the MAT and MAT&MSC analyses are exceptional; low COI pairwise substitution rates have been found in other insects, such as ants (1.5%, Quek *et al*., 2004) and *Drosophila* species (1.54%, Nunes *et al*., 2010), suggesting that caution should be exercised if calibrating the molecular clock according to the standard arthropod substitution rate of 2.3%.

Heled and Drummond (2010) highlighted the necessity of assessing multiple samples per species when inferring speciation times and that '*two or more sequences per species are necessary for a complete estimation of speciation times, given enough loci*'. We included from 4 to 18 sequences per species in our phylogenetic analyses with samples originating from different localities (except for *E. karyates* sp. n. that has only been recorded in Karyes of the Peloponnese, so all specimens were from one locality). Since the tree topology obtained from BEAST was congruent to those obtained from mitochondrial phylogenetic inferences (*i.e*., the COI dataset) and as the estimated molecular divergence times were concordant with the geological events that occurred in the Aegean region, we claim that our estimates for speciation events in the *E. minotaurus* group most likely reflect reality. Certainly, more sequences/taxa (or more loci) would further assist to elucidate the phylogeography of the *E. minotaurus* group but, unfortunately, insect sampling and gene amplification are always challenging.

Our phylogenetic assessment of the four species within the *E. minotaurus* group reflects their geographic distributions, with each species occurring in a specific region and belonging to a separate geographical cluster. As the initial diversification event occurred approximately 11.08 Mya (hereinafter, all timings are based on our MAT&MSC analysis), we speculate that there was a single species during the Miocene in Ägäis, which served as the first ancestor of all species of the *E. minotaurus* group (as it is known today). When the MAT occurred, eastern populations split from western ones, with one population progressively dominating the eastern part of the Aegean to become *E. crassus*. Our biogeographic reconstructions suggest an east-to-west (from the East Aegean towards the Greek mainland and the Balkan Peninsula) species diversification of *E. crassus*, with dispersal and/or vicariant events, confirming the MAT scenario. In the biogeographic context, the Greek mainland was isolated from Anatolia and the East Aegean Islands at 0.18-0.14 Mya (and were most likely consolidated until the end of the Pleistocene at 0.021 Mya), and some of the Aegean Islands started to acquire their current configurations ca. 0.03-0.018 Mya and were finally shaped at 0.008 Mya (for a thorough review see Kougioumoutzis *et al*., 2017). We have estimated speciation of *E. crassus* at 0.91 Mya (mid-Pleistocene), reflecting a period of momentous geological and climatic changes in the Aegean that likely drove speciations and/or extinctions.

Another diversification event was detected at 7.6 Mya by our analyses that separated a north-western population (Balkan Peninsula) from a south-western one (Peloponnese/ Crete and Karpathos); our biogeographic analyses confirmed that 'north-to-south' division. Distribution patterns among the Aegean Islands are far more complex than those of the Ionian Islands because of their greater numbers and greater topographic, palaeogeographic, and environmental complexity (Gillespie and Clague, 2009; Kougioumoutzis *et al*., 2017). However, "*the fauna and flora in the Ionian Islands are expected to be more 'harmonic', without profound gaps in their taxonomic composition*" (Gillespie and Clague, 2009), harbouring fewer endemic taxa and existing taxa being more similar to those of the adjacent mainland. Indeed, *E. phaeacus* sp. n. is an insular (Corfu: Ionian Archipelago, Greece) and montane species (Balkan Peninsula: Mt Olympus, Greece; and Mt Rumija, Montenegro). Speciation forces similar to those that acted on *E. crassus* must have also influenced speciation of *E. phaeacus* sp. n. (estimated divergence at 0.67 Mya).

The Messinian Salinity Crisis was another major event that occurred in the Aegean, during which Crete became isolated from the Greek mainland but maintained a land connection to the Peloponnese until 5 Mya. Due to intense tectonic phenomena, the Aegean region was fragmented and considerably altered during the Pliocene. Crete became permanently isolated from the Peloponnese and other inland areas, and a wide sea-barrier (aka the Corinthian Channel) separated the Peloponnese from mainland Greece (5-3 Mya, Dermitzakis, 1990). Later, during the Pleistocene, climatic oscillations and sea-level fluctuations led to repeated connection/disconnection cycles (eight glacial cycles; for a review see Perissoratis and Conispoliatis, 2003), which altered the size and isolation of land areas (*e.g*. of the islands) by forming temporary land-

bridges/corridors, allowing exchange of biota between islands and the mainland. These sea-level fluctuations continued until the late Pleistocene (0.021 Mya) and into the Holocene (Dermitzakis, 1990), inducing species diversification and dispersal (Perissoratis and Conispoliatis, 2003). A diversification event occurred 5.2 Mya within the southern populations of the *E. minotaurus* complex that subsequently gave rise to two species: *E. karyates* sp. n. (Peloponnese cluster) and *E. minotaurus* (Crete and Karpathos cluster). We have estimated the speciation events for these latter two species to date to 0.49 Mya and 2.26 Mya, respectively. We speculate that gene flow between the Peloponnese and Crete/Karpathos populations was impeded at the end of the MSC, when the Mediterranean Sea was refilled, and that speciation was favoured when the sea level started to stabilize. It is worth mentioning that the disconnection of Crete and Karpathos Islands (5-2 Mya) did not seem to affect the distribution of *E. minotaurus* (the same species is recorded on both islands), and no further speciation has taken place.

Among other phylogeographic studies carried out in the Aegean that explore the driving forces of animal speciation and biogeographic patterns, Poulakakis (2014) highlighted the importance of MAT for species distributions in the area. According to that study, species such as those of the *E. minotaurus* group can be characterized as post-MAT colonizers, describing them as "*species that reached the region after the creation of the MAT, and whose diversification is due to the MSC, intense tectonism during the Pliocene and the climatic oscillations in these periods*" (Poulakakis *et al*., 2014). Molecular clock is infrequently applied to insects groups in the Aegean, and when it does, it concerns mostly beetles (Papadopoulou *et al*., 2009; 2010), crickets (Allegrucci *et al*., 2009; 2011), termites (Luchetti *et al*., 2005; 2007) and sand fly (Kasap *et al*., 2015). Here, for the first time, we present phylogeographic and mitochondrial dating inferences about the hoverfly genus *Eumerus* in the Aegean, firmly supported by integrative taxonomic data, which may foster similar studies on other hoverfly genera to further elucidate the biogeographic evolution of the Aegean.

Acknowledgements

The authors would like to thank three anonymous reviewers for their valuable comments and suggestions that improved the quality of this paper. We thank John O'Brien for proof reading and making constructive suggestions on the text. Financial support for this research was provided by the Serbian Ministry of Education, Science and Technological Development (Projects OI173002 and III43002) and the Provincial Secretariat for Science and Technological Development (Project 'Genetic resources of agro-ecosystems in Vojvodina and sustainable agriculture'), as well as the European Union (European Social Fund – ESF) and Greek national funds through the Operational Program 'Education and Lifelong Learning' of the National Strategic Reference Framework (NSRF) – Research Funding Program: THALES. Investing in knowledge society through the European Social Fund. We also acknowledge the Program «Grants IKY» of the State Scholarships Foundation of Greece, in the frame of the OP «Education and Lifelong Learning» of the European Social Fund (ESF) – NSRF, 2007–2013 (contract WP2-SHORT TERMS-19348) as partial financial support for the PhD thesis of AC.

References

Ačanski J, Vujić A, Djan M, Obreht Vidaković D, Ståhls G, Radenković S. 2016. Defining species boundaries in the *Merodon avidus* complex (Diptera, Syrphidae) using integrative taxonomy, with a description of a new species. *European Journal of Taxonomy* 237: 1-25.

Ačanski J. 2017. Taxonomy and distribution of the genus *Merodon* Meigen (Diptera: Syrphidae) in Palearctic. PhD thesis (in Serbian), University of Novi Sad, Novi Sad, pp 209.

Akin C, Can Bilgin C, Beerli P, Westaway R, Ohst T, Litvinchuk SN, Uzzell T, Bilgin M, Hotz H, Guex GD, Plötner J. 2010. Phylogeographic patterns of genetic diversity in eastern Mediterranean water frogs were determined by geological processes and climate change in the Late Cenozoic. *Journal of Biogeography* 37: 2111-2124.

Allegrucci G, Rampini M, Gratton P, Todisco V, Sbordoni V. 2009. Testing phylogenetic hypotheses for reconstructing the evolutionary history of *Dolichopoda* cave crickets in the eastern Mediterranean. *Journal of Biogeography* 36: 1785-1797.

Allegrucci G, Trucchi E, Sbordoni V. 2011. Tempo and mode of species diversification in *Dolichopoda* cave crickets (Orthoptera, Rhaphidophoridae). *Molecular Phylogenetics and Evolution* 60: 108-121.

Arnqvist G, Mårtensson T. 1998. Measurement error in geometric morphometrics: empirical strategies to assess and reduce its impact on measures of shape. *Acta Zoologica Academiae Scientiarum Hungaricae* 44: 73-96.

Arzone A. 1973. *Tragopon pratensis* L., ospite naturale di *Eumerus tricolor* Meigen (Dipt. Syrphidae). *Tipografia Vincenzo Bona, Torino* 8:55-66.

Arzone A. 1971. Reperti biologici su *Eumerus tricolor* Meigen, nocivo alle coltivazioni di *Tragopogon porrifolius* L. in

Piemonte (Dipt.Syrphidae). Tipografia Vincenzo Bona, Torino 7: 17-52.

Awasthi, M, Kashyap, A, Serajuddin, M. 2016. Molecular phylogeny of four gouramis based on divergent domain D11 of 28S rRNA gene. *Advances in Biological Research* 10: 351-353.

Ayres DL, Darling A, Zwickl DJ, Beerli P, Holder MT, Lewis PO, Huelsenbeck JP, Ronquist F, Swofford DL, Cummings MP, Rambaut A, Suchard MA. 2012. BEAGLE: an application programming interface and high-performance computing library for statistical phylogenetics. *Systematic Biology* 61: 170-173.

Baylac, M, Frieß, M. 2005. Fourier descriptors, Procrustes superimposition, and data dimensionality: an example of cranial shape analysis in modern human populations. *In Modern morphometrics in physical anthropology*. Springer, Boston, MA. 145-165.

Belshaw R, Fitton M, Herniou E, Gimeno C, Quicke DLJ. 1998. A phylogenetic reconstruction of the Ichneumonoidea (Hymenoptera) based on the D2 variable region of 28s ribosomal RNA. *Systematic Entomology* 23: 109-123.

Bickford D, Lohman DJ, Navjot SS, Ng PKL, Meier R, Winker K, Ingram KK, Das I. 2007. Cryptic species as a window on diversity and conservation. *Trends in Ecology and Evolution* 22: 148-155.

Bofkin L, Goldman N. 2007. Variation in evolutionary processes at different codon positions. *Molecular Biology and Evolution* 24: 513-521.

Bonelli S, Witek M, Canterino, S, Sielezneiew M, Stankiewicz-Fiedurek A, Tartally A, Balletto E, Schonrogge K. 2011. Distribution, host specificity, and the potential for cryptic speciation in hoverfly *Microdon myrmicae* (Diptera: Syrphidae), a social parasite of Myrmica ants. *Ecological Entomology* 36: 135-143.

Brower AVZ. 1994. Rapid morphological radiation and convergence among races of the butterfly *Heliconius erato* inferred from patterns of mitochondrial DNA evolution. *Proceedings of the National Academy of Sciences USA* 91: 6491-6495.

Brummitt RK, Pando F, Hollis S, Brummitt NA. 2001. World geographical scheme for recording plant distributions. International Working Group on Taxonomic Databases for Plant Sciences (TDWG).

Chen H, Rangasamy M, Tan SY, Wang HC, Siegfried BD. 2010. Evaluation of five methods for total DNA extraction from western corn rootworm beetles. *PLoS One* 5: 1-6.

Chroni A, Djan M, Vidaković DO, Petanidou T, Vujić A. 2017. Molecular species delimitation in the genus Eumerus (Diptera: Syrphidae). *Bulletin of Entomological Research* 107: 126-138.

Clement M, Posada D, Crandall KA. 2000. TCS: a computer program to estimate gene genealogies. *Molecular Ecology* 9: 1657-1660.

Cowling DE, Burnet B. 1981. Courtship songs and genetic control of their acoustic characteristics in sibling species of the *Drosophila melanogaster* subgroup. *Animal Behaviour* 29: 924-935.

Dayrat B. 2005. Towards integrative taxonomy.*Biological Journal of the Linnean Society* 85: 407-415.

Dell Statistica. 2015. Dell Statistica data analysis software system, version 13. Dell Inc.

Dermitzakis MD. 1990. Paleogeography, geodynamic processes and event stratigraphy during the Late Cenozoic of the Aegean area. *Accademia Nazionale dei Lincei* 85: 263-288.

Dias VS, Silva JG, Lima KM, Petitinga CSCD, Hernández-Ortiz V, Laumann RA, Paranhos BJ, Uramoto K, Zucchi RA, Joachim-Bravo IS. 2016. An integrative multidisciplinary approach to understanding cryptic divergence in Brazilian species of the *Anastrepha fraterculus* complex (Diptera: Tephritidae). *Biological Journal of the Linnean Society* 117: 725-746.

Diaz SA, Moncada LI, Murcia CH, Lotta IA, Matta NE, Adler PH. 2015. Integrated taxonomy of a new species of black fly in the subgenus *Trichodagmia* (Diptera: Simuliidae) from the Páramo Region of Colombia. *Zootaxa* 3914: 541-57.

Doczkal D. 1996. Description of two new species of the genus *Eumerus* Meigen (Dipt., Syrph.) from Corsica. *Volucella* 2: 3-19.

Drummond AJ, Suchard MA, Xie D, Rambaut A. 2012. Bayesian phylogenetics with BEAUti and the BEAST 1.7. *Molecular Biology and Evolution* 29: 1969-1973.

Folmer O, Black M, Hoeh W, Lutz R, Vrijenhoek R. 1994. DNA primers for amplification of mitochondrial cytochrome c oxidase subunit I from diverse metazoan invertebrates. *Molecular Marine Biology and Biotechnology* 3: 294-299.

Francuski L, Ludoški J, Vujić A, Milankov V. 2009. Wing geometric morphometric inferences on species delimitation and intraspecific divergent units in the *Merodon ruficornis* group (Diptera, Syrphidae) from the Balkan Peninsula. *Zoological Science* 26: 301-308.

Francuski L, Ludoški J, Vujić A, Milankov V. 2011. Phenotypic evidence for hidden biodiversity in the *Merodon aureus* group (Diptera, Syrphidae) on the Balkan Peninsula: conservation implication. *Journal of Insect Conservation* 15: 379-388.

Gillespie RG, Clague DA. 2009. *Encyclopedia of Islands*. No. 2.Univ of California Press.

Gkontas I, Papadaki S, Trichas A, Poulakakis N. 2016. First assessment on the molecular phylogeny and phylogeography of the species *Gnaptor boryi* distributed in Greece (Coleoptera: Tenebrionidae). *Mitochondrial DNA Part A* 1-8. http://dx.doi.org/10.1080/24701394.2016.1209196

Goloboff PA. 1999. NONA (NO NAME), version 2 [computer program]. Tucumán, Argentina: The Author.

Grković A, Vujić A, Radenković S, Chroni A, Petanidou T. 2015. Diversity of the genus *Eumerus* Meigen (Diptera, Syrphidae) on the eastern Mediterranean islands with description of three new species. *Annales de la Société Entomologique de France* 51: 361-373.

Grković A, Vujić A, Chroni A, van Steenis J, Đan M, Radenković S. 2017. Taxonomy and systematics of three species of the genus Eumerus Meigen, 1822 (Diptera: Syrphidae) new in southeastern Europe. *Zoologischer Anzeiger* 270: 176-192, https://doi.org/10.1016/j.jcz.2017.10.007

Hall TA. 1999. BioEdit: a user-friendly biological sequence alignment editor and analysis program for Windows 95/98/NT. *Nucleic Acids Symposium Series* 41: 95-98.

Hasson E, Soto IM, Carreira VP, Corio C, Soto EM, Betti M. 2009. Host plants, fitness and developmental instability in a guild of cactophilic species of the genus *Drosophila*. Pp. 89-109 in: Santos EB, ed., *Ecotoxicology Research Developments*. New York: Nova Science Publishers.

Hebert PD, Cywinska A, Ball SL, deWaard JR. 2003. Biological

identifications through DNA barcodes. *Proceedings of the Royal Society B* 270: 313-321.

Heled J, Drummond AJ. 2010. Bayesian inference of species trees from multilocus data. *Molecular Biology and Evolution* 27: 570-580.

Hijmans RJ, Cameron SE, Parra JL, Jones PG, Jarvis A. 2005. Very high resolution interpolated climate surfaces for global land areas. *International Journal of Climatology* 25: 1965-1978.

House CM, Lewis Z, Hodgson DJ, Wedell N, Sharma MD, Hunt J, Hosken DJ. 2013. Sexual and natural selection both influence male genital evolution. *PLoS One* 8: e63807. https://doi.org/10.1371/journal.pone.0063807

Huelsenbeck JP, Ronquist F. 2001. MRBAYES: bayesian inference of phylogenetic trees. *Bioinformatics* 17: 754-755.

Hurkmans W. 1993. A monograph of *Merodon* (Diptera: Syrphidae). Part 1. *Tijdschrift voor Entomologie* 136: 147-234.

Huson DH, Bryant D. 2006. Application of phylogenetic networks in evolutionary studies, *Molecular Biology and Evolution* 23: 254-267.

Kamilari M, Klossa Kilia E, Kilias G, Sfenthourakis S. 2014. Old Aegean palaeoevents driving the diversification of an endemic isopod species (Oniscidea, Trachelipodidae). *Zoologica Scripta* 43: 379-92.

Kasap OE, Dvorak V, Depaquit J, Alten B, Votypka J, Volf P. 2015. Phylogeography of the subgenus *Transphlebotomus Artemiev* with description of two new species, *Phlebotomus anatolicus* n. sp. and *Phlebotomus killicki* n. sp. *Infection, Genetics and Evolution* 34: 467-79.

Kasapidis P, Magoulas A, Mylonas M, Zouros E. 2005. The phylogeography of the gecko *Cyrtopodion kotschyi* (Reptilia: Gekkonidae) in the Aegean Archipelago. *Molecular Phylogenetics and Evolution* 35: 612-623.

Katoh K, Kuma K, Toh H, Miyata T. 2005. MAFFT version 5: improvement in accuracy of multiple sequence alignment. *Nucleic Acids Research* 33: 511-518.

Kirichenko N, Huemer P, Deutsch H, Triberti P, Rougerie R, Lopez-Vaamonde C. 2015. Integrative taxonomy reveals a new species of *Callisto* (Lepidoptera, Gracillariidae) in the Alps. *ZooKeys* 473: 157-176.

Klingenberg CP. 2011. MORPHOJ: an integrated software package for geometric morphometrics. Ver.2.0. *Molecular Ecology Resources* 11: 353-357.

Kougioumoutzis K, Valli AT, Georgopoulou E, Simaiakis S, Triantis KA, Trigas P. 2017. Network biogeography of a complex island system: the Aegean archipelago revisited. *Journal of Biogeography* 44: 651-660.

Librado P, Rozas J. 2009. DnaSP v5: a software for comprehensive analysis of DNA polymorphism data. *Bioinformatics* 25: 1451-1452.

Luchetti A, Marini M, Mantovani B. 2005. Mitochondrial evolutionary rate and speciation in termites: data on European *Reticulitermes* taxa (Isoptera, Rhinotermitidae). *Insectes Sociaux* 52: 218-221.

Luchetti A, Marini M, Mantovani B. 2007. Filling the European gap: biosystematics of the eusocial system *Reticulitermes* (Isoptera, Rhinotermitidae) in the Balkanic Peninsula and Aegean area. *Molecular Phylogenetics and Evolution* 45: 377-383.

Ludoški J, Francuski L, Vujić A, Milankov V. 2008. The *Cheilosia canicularis* group (Diptera: Syrphidae): species delimitation and evolutionary relationships based on wing geometric morphometrics. *Zootaxa* 1825: 40-50.

Mantel NA. 1967. The detection of disease clustering and a generalized regression approach. *Cancer Research* 27: 209-220.

Markov Z, Nedeljković Z, Ricarte A, Vujić A, Jovičić S, Józan Z, Mudri-Stojnić S, Radenković S, Ćetković A. 2016. Bee (Hymenoptera: Apoidea) and hoverfly (Diptera: Syrphidae) pollinators in Pannonian habitats of Serbia, with a description of a new *Eumerus* Meigen species (Syrphidae). *Zootaxa* 4154: 027-050.

Martinsson S, Erséus C. 2017. Cryptic speciation and limited hybridization within *Lumbricus earthworms* (Clitellata: Lumbricidae). *Molecular Phylogenetics and Evolution* 106:18-27.

Menezes BF, Vigoder FM, Peixoto AA, Varaldi J, Bitner-Mathé BC. 2013. The influence of male wing shape on mating success in *Drosophila melanogaster*. *Animal Behaviour* 85: 1217-1223.

Mengual, X, Ståhls, G, Rojo, S. 2008. First phylogeny of predatory flower flies (Diptera, Syrphidae, Syrphinae) using mitochondrial COI and nuclear 28S rRNA genes: conflict and congruence with the current tribal classification. *Cladistics* 24: 543-562.

Mezey JG, Houle D. 2005. The dimensionality of genetic variation for wing shape in *Drosophila melanogaster*. *Evolution* 59: 1027-1038.

Milankov V, Ludoški J, Ståhls G, Stamenković J, Vujić A. 2009. High molecular and phenotypic diversity in the *Merodon avidus* complex (Diptera, Syrphidae): cryptic speciation in a diverse insect taxon. *Zoological Journal of the Linnean Society* 155: 819-833.

Miller MA, Pfeiffer W, Schwartz T. 2010. Creating the CIPRES Science Gateway for inference of large phylogenetic trees. In: 2010 *Gateway Computing Environments Workshop*, GCE 2010.

Moraes EM, Manfrin MH, Laus AC, Rosada RS, Bomfin SC, Sene FM. 2004.Wing shape heritability and morphological divergence of the sibling species *Drosophila mercatorum* and *Drosophila paranaensis*. *Heredity* 92: 466-473.

Nedeljković Z, Ačanski J, Vujić A, Obreht D, Dan M, Ståhls G, Radenković S. 2013. Taxonomy of *Chrysotoxum festivum* Linnaeus, 1758 (Diptera: Syrphidae) – an integrative approach. *Zoological Journal of the Linnean Society* 169: 84-102.

Nedeljković Z, Ačanski J, Dan M, Obreht-Vidaković D, Ricarte A, Vujić A. 2015. An integrated approach to delimiting species borders in the genus *Chrysotoxum* Meigen, 1803 (Diptera: Syrphidae), with description of two new species. *Contributions to Zoology* 84: 285-304.

Nixon KC. 2002. WinClada ver. 1.00.08. Published by author, Ithaca, NY.

Nunes MD, Orozco-Ter Wengel PA, Kreissl M, Schlötterer C. 2010. Multiple hybridization events between *Drosophila simulans* and *Drosophila mauritiana* are supported by mtDNA introgression. *Molecular Ecology* 19: 4695-707.

Outomuro D, Adams DC, Johansson F. 2013. The evolution of wing shape in ornamented-winged damselflies (Calopterygidae, Odonata). *Evolutionary biology* 40: 300-309.

Padial JM, Miralles A, de la Riva I, Vences M. 2010. The

integrative future of taxonomy. *Frontiers in Zoology* 7: 16.

Papadopoulou A, Anastasiou I, Keskin B, Vogler AP. 2009. Comparative phylogeography of tenebrionid beetles in the Aegean archipelago: the effect of dispersal ability and habitat preference. *Molecular Ecology* 18: 2503-2517.

Papadopoulou A, Anastasiou I, Vogler AP. 2010. Revisiting the insect mitochondrial molecular clock: the mid-Aegean trench calibration. *Molecular Biology and Evolution* 27: 1659-1672.

Papakostas S, Michaloudi E, Proios K, Brehm M, Verhage L, Rota J, Peña C, Stamou G, Pritchard VL, Fontaneto D, Declerck SAJ. 2016. Integrative taxonomy recognizes evolutionary Units despite widespread mitonuclear discordance: evidence from a rotifer cryptic species complex. *Systematic Biology* 65: 508-524.

Pape T, Thompson FC (eds). 2015. Systema Dipterorum. Version 1.5.Available online at http://www.diptera.org/

Parmakelis A, Stathi I, Chatzaki M, Simaiakis S, Spanos L, Louis C, Mylonas M. 2006. Evolution of *Mesobuthus gibbosus* (Brulle, 1832) (Scorpiones: Buthidae) in the northeastern Mediterranean region. *Molecular Ecology* 15: 2883-2894.

Perez MF, Carstens BC, Rodrigues GL, Moraes EM. 2016. Anonymous nuclear markers data supporting species tree phylogeny and divergence time estimates in a cactus species complex in South America. *Data Brie*f 6: 456-460.

Pérez-Bañón C, Marcos-García A. 1998. Life history and description of the immature stages of *Eumerus purpurariae* (Diptera: Syrphidae) developing in *Opuntia maxima*. *European Journal of Entomology* 95: 373-82.

Pérez-Ponce de León G, Nadler SA. 2010. What we don't recognize can hurt us: A plea for awareness about cryptic species. *Journal of Parasitology* 96: 453-464.

Perissoratis C, Conispoliatis N. 2003. The impacts of sea-level changes during latest Pleistocene and Holocene times on the morphology of the Ionian and Aegean seas (SE Alpine Europe). *Marine Geology* 196: 145-156.

Petanidou T, Vujić A, Ellis WN. 2011. Hoverfly diversity (Diptera: Syrphidae) in a Mediterranean scrub community near Athens, Greece. *Annales de la Société Entomologique de France* 47: 168-175.

Pfenninger M, Schwenk K. 2007. Cryptic animal species are homogeneously distributed among taxa and biogeographical regions. *Journal of Evolutionary Biology* 7: 121.

Popović D, Ačanski J, Djan M, Obreht D, Vujić A, Radenković S. 2015. Sibling species delimitation and nomenclature of the *Merodon avidus* complex (Diptera: Syrphidae). *European Journal of Entomology* 112: 790-809.

Posada D, Crandall KA. 2001. Evaluation of methods for detecting recombination from DNA sequences: computer simulations. *Proceedings of the National Academy of Sciences USA* 98: 13757-13762.

Poulakakis N, Lymberakis P, Valakos E, Pafilis P, Zouros E, Mylonas M. 2005. Phylogeography of Balkan wall lizard (*Podarcis taurica*) and its relatives inferred from mitochondrial DNA sequences. *Molecular Ecology* 14: 2433-2443.

Poulakakis N, Sfenthourakis S. 2008. Molecular phylogeny and phylogeography of the Greek populations of the genus *Orthometopon* (Isopoda, Oniscidea) based on mitochondrial DNA sequences. *Zoological Journal of the Linnean Society* 152: 707-715.

Poulakakis N, Kapli P, Lymberakis P, Trichas A, Vardinoyiannis K, Sfenthourakis S, Mylonas M. 2015. A review of phylogeographic analyses of animal taxa from the Aegean and surrounding regions. *Journal of Zoological Systematics and Evolutionary Research* 53: 18-32.

Puillandre N, Stöcklin R, Favreau P, Bianchi E, Perret F, Rivasseau A, Limpalaër L, Monnier E, Bouchet P. 2014. When everything converges: Integrative taxonomy with shell, DNA and venomic data reveals *Conus conco*, a new species of cone snails (Gastropoda: Conoidea). *Molecular Phylogenetics and Evolution* 80: 186-92.

Quantum GIS Development Team. 2012. Quantum GIS Geographic Information System. Version 2.12.3 Lyon [Internet]. Open Source Geospatial Foundation Project, available at http://qgis.osgeo.org.

Quek SP, Davies SJ, Itino T, Pierce NE. 2004. Codiversification in an ant-plant mutualism: stem texture and the evolution of host use in *Crematogaster* (Formicidae: Myrmicinae) inhabitants of Macaranga (Euphorbiaceae). *Evolution* 58: 554-70.

Radenković S, Šašić Zorić L, Djan M, Obreht Vidaković D, Ačanski J, Ståhls G, Veličković N, Markov Z, Petanidou T, Kočiš Tubić N, Vujić A. 2017. Cryptic speciation in the *Merodon luteomaculatus* complex (Diptera: Syrphidae) from the eastern Mediterranean. *Journal of Zoological Systematics and Evolutionary Research*: 1-22.

Rambaut A. 2013. FigTree, http://tree.bio.ed.ac.uk/software/figtree/

Rambaut A, Suchard MA, Xie D, Drummond AJ. 2014. Tracer v1.6. http://tree.bio.ed.ac.uk/software/tracer/

Rambaut A, Lam TT, Carvalho LM, Pybus OG. 2016. Exploring the temporal structure of heterochronous sequences using TempEst (formerly Path-O-Gen). *Virus Evolution* 2: vew007.

Ratnasingham S, Hebert PDN. 2013. A DNA-based registry for all animal species: the Barcode Index Number (BIN) system. *PLoS ONE* 8: e66213.

Rato C, Harris DJ, Carranza S, Machado L, Perera A. 2016. The taxonomy of the *Tarentola mauritanica* species complex (Gekkota: Phyllodactylidae): Bayesian species delimitation supports six candidate species. *Molecular Phylogenetics and Evolution* 94: 271-278.

Ricarte A, Nedeljković Z, Rotheray GE, Yszkowski RM, Hancock EG, Watt K, Hewitt SM, Horsefield D, Wilkinson G. 2012. Syrphidae (Diptera) from the Greek island of Lesvos, with description of two new species. *Zootaxa* 317:1-23.

Rodriguez F, Oliver JL, Marin A, Medina JR. 1990. The general stochastic-model of nucleotide substitution. *Journal of Theoretical Biology* 142: 485-501.

Rohlf FJ. 2006. TpsDig-Digitize landmarks and outlines. Ver.2.05. New York: Department of Ecology and Evolution, State University of New York at Stony Brook.

Rohlf FJ, Slice DE. 1990. Extensions of the Procrustes method for the optimal superimposition of landmarks. *Systematic Zoology* 39: 40-59.

Ronquist F, Huelsenbeck JP. 2003. MrBayes3: Bayesian phylogenetic inference undermixed models. *Bioinformatics* 19: 1572-1574.

Rosenberg MS, Anderson CD. 2011. PASSaGE: Pattern Analysis, Spatial Statistics and Geographic Exegesis. Version 2. *Methods in Ecology and Evolution* 2: 229-232.

Rotheray GE, Gilbert F. 2011. *The Natural History of Hoverflies*. UK, Ceredigion.

Routtu J, Mazzi D, Van Der Linde K, Mirol P, Butlin RK, Hoikkala A. 2007. The extent of variation in male song, wing and genital characters among allopatric *Drosophila montana* populations. *Journal of evolutionary biology* 20: 1591-1601.

Sacchi R, Hardersen S. 2013. Wing length allometry in *Odonata*: differences between families in relation to migratory behaviour. *Zoomorphology* 132: 23-32.

Šašić L, Ačanski J, Vujić A, Ståhls G, Radenković S, Milić D, Vidaković DO, Đan M. 2016. Molecular and morphological inference of three cryptic species within the *Merodon aureus* species group (Diptera: Syrphidae). *PLoS ONE* 11: e0160001.

Schlick-Steiner BC, Steiner FM, Seifert B, Stauffer C, Christian E, Crozier RH. 2010. Integrative taxonomy: a multisource approach to exploring Biodiversity. *Annual Review of Entomology* 55: 421-438.

Sfenthourakis S, Triantis KA. 2017. The Aegean archipelago: a natural laboratory of evolution, ecology and civilisations. *Journal of Biological Research-Thessaloniki* 24: 4.

Shapiro B, Rambaut A, Drummond AJ. 2006. Choosing appropriate substitution models for the phylogenetic analysis of protein-coding sequences. *Molecular Biology and Evolution* 23: 7-9.

Sheets HD. 2012. IMP software series. Buffalo, New York: Canisius College.

Simaiakis SM, Dimopoulou A, Mitrakos A, Mylonas M, Parmakelis A. 2012. The evolutionary history of the Mediterranean centipede *Scolopendra cingulata* (Latreille, 1829) (Chilopoda: Scolopendridae) across the Aegean archipelago. *Biological Journal of the Linnean Society* 105: 507-521.

Simmons MP, Zhang LB, Webb CT, Reeves A. 2006. How can third codon positions outperform first and second codon positions in phylogenetic inference? An empirical example from the seed plants. *Systematic Biology* 55: 245-58.

Simon C, Frati F, Beckenbach A, Crespi B, Liu H, Flook P. 1994. Evolution, weighting, and phylogenetic utility of mitochondrial gene-sequences and a compilation of conserved polymerase chain-reaction primers. *Annals of the Entomological Society of America* 87: 651-701.

Smit JT, van Harten A, Ketelaar R. 2017. The hoverflies of the Arabian Peninsula. In: Arthropod fauna of the UAE, Chapter: Order Diptera, Family Syrphidae. Eds. Tony van Harten, 572-612.

Soldati L, Kergoat GJ, Clamens AL, Jourdan H, Jabbour-Zahab R, Condamine FL. 2014. Integrative taxonomy of New Caledonian beetles: species delimitation and definition of the *Uloma isoceroides* species group (Coleoptera, Tenebrionidae, Ulomini), with the description of four new species. *ZooKeys* 415: 133-167.

Speight MCD, Hauser M, Withers P. 2013. *Eumerus narcissi* Smith (Diptera, Syrphidae), presence in Europe confirmed, with a redescription of the species. *Dipterist Digest* 20: 17-32.

Speight, MCD 2016. Species accounts of European Syrphidae (Diptera). Syrph the Net, the database of European Syrphidae. Dublin. 93: Syrph the Net publications pp. 288.

Stackelberg AA. 1961. Palaearctic species of the genus *Eumerus* Mg. (Diptera, Syrphidae). *Trudy Vsesojuznogo Entomologiceskogo Obscestva* 48, 181-229.

Stamatakis A. 2006. RAxML-VI-HPC: Maximum likelihood-based phylogenetic analyses with thousands of taxa and mixed models. *Bioinformatics* 22: 2688-2690.

Stamatakis A, Hoover P, Rougemont J. 2008.A rapid bootstrap algorithm for the RAxML Web servers. *Systematic Biology* 57: 758-71.

Strasser TF, Panagopoulou E, Runnels CN, Murray PM, Thompson N, Karkanas P, McCoy FW, Wegmann KW. 2010. Stone Age seafaring in the Mediterranean: evidence from the Plakias region for lower palaeolithic and mesolithic habitation of Crete. *Hesperia* 79: 145-190.

Strid A. 2016. Atlas of the Aegean flora. *Englera* 33: 1-578.

Stubbs AE, Falk S. 1983. *British hoverflies: an illustrated guide*. British Entomological and Natural History Society, London.

Tamura K, Stecher G, Peterson D, Filipski A, Kumar S. 2013. MEGA6: Molecular Evolutionary Genetics Analysis Version 6.0. *Molecular Biology and Evolution* 30: 2725-2729.

Thompson CF. 1999. A key to the genera of the flower flies (Diptera: Syrphidae) of the Neotropical Region including descriptions of new genera and species and a glossary of taxonomic terms. *Contributions on Entomology International* 3: 319-378.

van Steenis J, Hauser M, van Zuijen MP. 2017. Review of the *Eumerus barbarus* species group (Diptera: Syrphidae) from the western Mediterranean Basin. *Bonn Zoological Bulletin* 66: 145-165.

Vujić A, Ståhls G, Ačanski J, Bartsch H, Bygebjerg R, Stefanović A. 2013. Systematics of *Pipizini* and taxonomy of European Pipiza Fallen: molecular and morphological evidence (Diptera, Syrphidae). *Zoologica Scripta* 42: 288-305.

Vujić A, Radenković S, Ačanski J, Grković A, Taylor M, Şenol SG, Hayat R. 2014. Revision of the species of the *Merodon nanus* group (Diptera: Syrphidae) including three new species. *Zootaxa* 4006: 439-462.

Yeaman S, Chen Y, Whitlock MC. 2010. No effect of environmental heterogeneity on the maintenance of genetic variation in wing shape in *Drosophila melanogaster*. *Evolution* 64: 3398-3408.

Yu Y, Harris AJ, Blair C, He XJ. 2015. RASP (Reconstruct Ancestral State in Phylogenies): a tool for historical biogeography. *Molecular Phylogenetics and Evolution* 87: 46-49.

Zelditch ML, Swiderski DL, Sheets HD, Fink WL. 2004. *Geometric morphometrics for biologists: a primer*. London: Elsevier Academic Press.

Zhang JJ, Kapli P, Pavlidis P, Stamatakis A. 2013. A general species delimitation method with applications to phylogenetic placements. *Bioinformatics* 29: 2869-2876.

Received: 5 March 2018
Revised and accepted: 7 August 2018
Published online: 2 November 2018
Editor: A. Ivanović

Online supplementary information

S1. List of specimens used for wing geometric morphometric analysis by geographical area and species.

S2. Maximum likelihood analysis for the concatenated 3' and 5' fragments of the COI gene (COI dataset). Values above branches indicate bootstrap replicates (only values >50 are illustrated).

S3. Neighbor-joining analysis for the concatenated 3' and 5' fragments of the COI gene (COI dataset). Values in the branches indicate bootstrap replicates (only values >50 are illustrated).

S4. Bayesian analysis for the concatenated 3' and 5' fragments of the COI gene (COI dataset). Values indicate Bayesian probabilities.

S5. Haplotype networks constructed using the statistical parsimony algorithm for the concatenated 3' and 5' fragments of the COI gene (COI subset) for the *E. minotaurus* group.

S6. Maximum parsimony analysis of the 28S gene fragment (28S dataset). Only one tree was generated (Length 90 steps, CI=93, RI=81). Filled circles denote unique changes and open circles are non-unique changes. Bootstrap support values are illustrated above the branches.

S7. Results of Principal component analysis conducted on wing shape variables.

S8. Results of discriminant analysis conducted on wing shape variables. F values are shown above the diagonal, p values are shown below the diagonal (df = 13.35).

Appendix

Systematics

Eumerus minotaurus group

Diagnosis. Species with elongated pedicel, at least 1.5 times longer than deep. Short body pile. Metafemur moderately swollen. Ventral pile on metafemur not longer than half the depth of the femur. Abdomen black with bronze to gold tinge laterally, about two times as long as wide. S4 in males flat, with invaginated posterior margin (Figure 10K), very similar in shape in all species of the group. Posterior surstyle lobe in males genitalia simple, oval (Figure 10A-C); hardly varying in shape between species, except for *E. crassus* and *E. niehuisi* (slightly different). The group includes the following species in Europe: *E. crassus* (Figure 11E), *E. longicornis* (Figures 10B, E, M, 11F), *E. niehuisi* and the *E. minotaurus* cryptic species complex (comprising *E. karyates* sp. n., *E. minotaurus* and *E. phaeacus* sp. n.; hereafter named *E. minotaurus* complex); and in Turkey: *E. anatolicus* sp. n. and *E. crassus*.

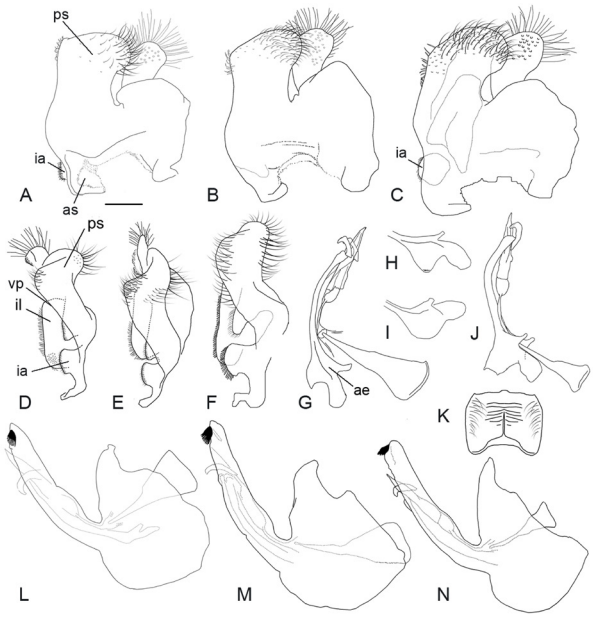

Figure 10. Male genitalia. Epandrium, lateral view: A) *E. minotaurus* complex, B) *E. longicornis* Loew, 1855, C) *E. anatolicus* sp. n., ventral view: D) *E. minotaurus* complex, E) *E. longicornis*, F) *E. anatolicus* sp. n.; G) *E. minotaurus* Claussen and Lucas, 1988, aedeagus with accessory structures; distal part of aedeagal apodeme: H) *E. karyates* sp. n., I) *E. phaeacus* sp. n., J) *E. anatolicus* sp. n., aedeagus with accessory structures; K) *E. minotaurus* complex, males abdominal sternite IV; hypandrium, lateral view: L) *E. minotaurus* complex, M) *E. longicornis*, N) *E. anatolicus* sp. n. Scale 0.2 mm. ae – aedeagal apodeme, as – anterior lobe of surstylus, il – interior lobe of posterior lobe of surstylus, ia – inner lobe of anterior lobe of surstylus, ps – posterior lobe of surstylus, vp – ventral margin of posterior surstyle lobe.

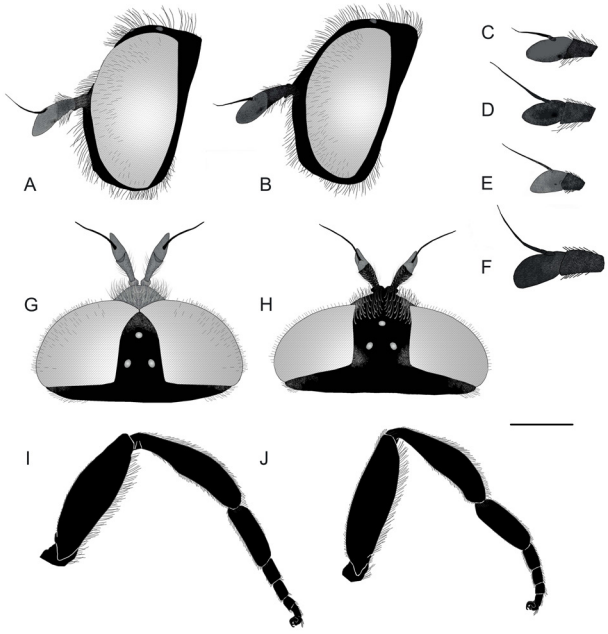

Figure 11. *E. minotaurus* group, head, lateral view: A) *E. minotaurus* Claussen and Lucas, 1988, male, B) *E. phaeacus* sp. n., female; antenna: C) *E. karyates* sp. n., D) *E. anatolicus* sp. n., E) *E. crassus* Grković, Vujić and Radenković, 2015, F) *E. longicornis* Loew, 1855; dorsal view: G) *E. minotaurus*, male, H) *E. phaeacus* sp. n., female. *E. minotaurus* complex, leg: I) male, J) female. Scale: 1mm.

Eumerus minotaurus cryptic species complex

Diagnosis. Dark appearance, body blackish-bronze. Eyes covered with long white scattered pilosity (Figure 11G, H), whereas eyes in *E. longicornis* are almost bare. Second and third antennal segment elongated, with almost the same width (Figure 11A-C), similar to *E. longicornis* but the ventral margin of the basoflagellomere of this latter species is linear (Figure 11F) whereas it is slightly convex in the *E. minotaurus* complex. White to grey, very narrow and linear pollinose maculae on tergites, often absent on T4, especially among female; these maculae are well expressed and lunulate in *E. longicornis* in particular, but also in other species of the *E. minotaurus* group. Females of the *E. minotaurus* complex can be easily

Table 5. Morphological differences between the *E. minotaurus* complex and *E. longicornis*.

E. longicornis Loew, 1855	*E. minotaurus* complex
Eyes almost bare	Eyes covered with moderately long and dense pile
Ventral margin of basoflagellomere linear	Ventral margin of basoflagellomere slightly convex
Ventral pile of pedicel shorter than the depth of pedicel	Ventral pile of pedicel longer than the depth of pedicel
Ventral pile of scape distinctly longer than ventral pile of pedicel	Ventral pile of scape about the same length as ventral pile of pedicel
Ventral pile on femur short as the dorsal	Ventral pile on femur longer than the dorsal
Pollinose maculae on tergites II–IV wide, well expressed, third pair clearly oblique	Pollinose maculae on tergites II–IV narrow, linear, third pair often absent

distinguished from *E. crassus* females by the well-developed and wider pairs of maculae on T2-4 and the conspicuously developed pollinosity behind the posterior ocellus of *E. crassus*. Table 5 describes the clear morphological differences between the *E. minotaurus* complex and *E. longicornis*. The male genitalia of these two taxa are shown in Figure 10.

Distribution. Eastern Mediterranean (Greece, Montenegro).

General description. *Male*. *Head*. Eyes holoptic. Eye contiguity about 6 ommatidia long. Eye with scattered long white pilosity, bare near the margins. Face, vertex and occiput black to bronze, moderately punctuated. Face with uneven white to bronze pollinosity, less or more expressed but usually with a prominent longitudinal median stripe of silver pollinosity. Ocellar triangle isosceles, longer than wide (Figure 11G). Face slightly convex, covered with white pile (Figure 11A). Pile on vertex and occiput yellow, but in ocellar triangle mixed with black. Scape and pedicel dark brown and covered with yellow pile, ventrally as long as the depth of the pedicel. Pedicel elongated, almost as long as the basoflagellomere (Figure 11A-C). Basoflagellomere elongated, brown, from almost yellow to dark brown, covered with grey pollinosity. Sensory pit located ventrally near the distal margin of the basoflagellomere. Arista reddish-brown.

Thorax. Scutum, scutellum and pleurae black to bronze, moderately punctuated. Mesonotum anteriorly with fine white pollinosity that extends in two pollinose vittae, reaching 2/3 of the length of the scutum. Median vitta present only in anterior part. Pile on thorax yellow to white, short on scutum and scutellum and longer on pleurae. Pleurae black with bronze to golden sheen, covered in silvery-white pollinosity and long white pile. Scutellum roughly transversely striated. Legs black to brown with reddish connections between segments, covered with golden pollinosity and moderately long white pile (Figure 11I). Metatrochanter covered in medium length pile. Metafemur moderately swollen, ventral pile yellow to white, as long as about half the depth of the femur. Metatibia greatly thickened, a little narrower than metafemur, slightly curved. Tarsi covered with short, dense, golden pile ventrally. Plumula covered in dark yellow pilosity. Wing with brown tinge. Costal bristles black.

Abdomen. Length: width of abdomen is about 1.4-1.6. Tergites black, densely punctuated, covered in short white pilosity that turns yellow in proximal half of T4. T1 with scarce white pollinosity laterally. T2-3 with pairs of silvery-white maculae of pollinosity, narrow, almost straight. Maculae on T4 barely visible, sometimes absent. Sternites light brown, covered with bronze pollinosity and moderately long white to yellow pile. S3 wide, on posterior margin with longer yellow to golden pile. Pregenital segment covered with golden pilosity.

Male genitalia. Posterior surstyle lobe large, covered with long scattered pile (Figure 10A, D). IL covered with short dense pilosity (Figure 10D). Hypandrium simple (Figure 10L). Distal part of aedeagal apodeme with processes that differ in shape in different species of the *E. minotaurus* complex (Figure 10G-I).

Female. Similar to the male with normal sexual dimorphism (Figure 11B, H, J). Frons less or more wrinkled longitudinally, in narrower part approximately as wide as one fourth of the width of the head in dorsal view or twice as wide as the width of the ocellar triangle. White pollinosity along eye margin less or more expressed. Pollinose maculae on T4 usually absent.

We have resolved three cryptic species within the *E. minotaurus* complex: *E. karyates* sp. n., *E. minotaurus* and *E. phaeacus* sp. n.

Eumerus minotaurus Claussen and Lucas, 1988

Material studied. Paratypes. One male, Greece: Crete, one male, Lasithi, Sissi, 08.iv.1983, leg. Claussen; Heraclion, 7.iv.1975, leg. Lucas, (NBC). Additional material. Greece: one female, Crete, Rethimnon, Bali, 06.v.2003, leg. Tkalcu; one female, Orne-Agia Galini, 25.iv.2014, leg. Vujić; 2 males, Fotinos, 26.v.2014, leg. Vujić; Chania, one male, Armeni, 25.iv.2014, leg. Vujić; one female, Imbors, 27.v.2014, leg. Vujić; one male, one female, Omalos plain, 28.v.2014, leg. Vujić; Karpathos, one male, Avlona, 02-04.v.2012, leg. Vavitsas.
Diagnosis. Differs from other species of the *E. minotaurus* complex by the shape of the distal part of the aedeagal apodeme (Figure 10G), wing morphometric characters (significant wing shape differences), and molecular data (see accession numbers in Appendix). Basoflagellomere is usually pointed (Figure 11A).
Distribution. Greece: Crete and Karpathos.
Description. Size: body length 10-11.5 mm; wing length 7-9 mm.
Male. Width of face: width of head is 0.25-0.3. Width of vertex: width of the head is 0.21-0.22. Length of eye contiguity: length of frons is 0.47-0.62. Basoflagellomere usually conspicuously pointed (Figure 11A). Width of pedicel: width of basoflagellomere is about 0.8. Width of pedicel: length of pedicel is about 0.6. Thorax. Length: width of scutellum is 0.5.
Female. Width of frons: width of head is 0.24-0.27. Width of pedicel: width of basoflagellomere is about 0.94. Width of pedicel: length of pedicel is 0.5-0.8. Abdomen. Height: width ratio of T4 is 0.8. Height: width of T3 is 0.46-0.49.

Eumerus karyates Chroni, Grković and Vujić sp. n.

Type material. Holotype. Male. Greece: Peloponnese, Karyes, 20.v.2016, legs. Vujić, Nedeljković, Ačanski, Likov, Miličić. Paratypes. Greece: Peloponnese, Karyes, three females, 20.v.2016; one male, 22.v.2016; two males, two females, 23.v.2016, legs. Vujić, Nedeljković, Ačanski, Likov, Miličić.
Diagnosis. Differs from other species of the *E. minotaurus* complex by the shape of the distal part of the aedeagal apodeme (Figure 10H), wing morphometric characters (significant wing shape differences) and molecular data (see accession numbers in Appendix). Basoflagellomere is slightly pointed, but less pronounced than in *E. minotaurus* (Figure 11C).
Distribution. Greece: Peloponnese.
Description. Size: body length 10-11 mm; wing length 7-8 mm.
Male. Head. Width of face: width of head is 0.27-0.32. Width of vertex: width of the head is 0.19-0.21. Length of eye contiguity: length of frons is 0.29-0.42. Basoflagellomere usually slightly pointed (Figure 11C). Width of pedicel: width of basoflagellomere is 0.8-0.9. Width of pedicel: length of pedicel is about 0.7. Thorax. Length: width of scutellum is 0.6.
Female. Head. Width of frons: width of head is 0.24-0.27. Width of pedicel: width of basoflagellomere is 0.8-1. Width of pedicel: length of pedicel is about 0.7. Abdomen. Height: width of T4 is 0.7. Height: width of T3 is 0.46.
Etymology. Karyatides are mainly known as the model figures sculptured as columns of the Erechtheion on the Acropolis of Athens and were the priestesses of Artemis at Karyae (today's Karyes) in ancient Laconia, Peloponnese. As all our Peloponnesian specimens derived from Karyes, we considered the male adjective "karyates" to be an appropriate name for the species.

Eumerus phaeacus Chroni, Grković and Vujić sp. n.

Type material. Holotype. Male. Greece: Corfu, Ano Korakiana, 24.v.2016, leg. Vujić, Nedeljković, Ačanski, Likov, Miličić. Paratypes. Montenegro, Rumija, one male, 42.11201 Lat., 111.217311 Long., 02.v.2011, leg. Vujić; Greece: Mt Olympus, one male, one female, Ag. Paraskevi, 17.v.2011, leg. Vujić; Corfu, Ano Korakiana, 14 males, 24.v.2016, leg. Vujić, Nedeljković, Ačanski, Likov, Miličić; four males, one female, Liapades, 24.v.2016, leg. Vujić, Nedeljković, Ačanski, Likov, Miličić; one male, Strinilas, 24.v.2016, leg. Vujić, Nedeljković, Ačanski, Likov, Miličić.
Diagnosis. Differs from other species of the *E. minotaurus* complex by the shape of the distal part of the aedeagal apodeme (Figure 10I), the absence of pollinosity behind the posterior ocelli, wing morphometric characters (significant wing shape differences) and molecular data (see accession numbers in Appendix). Basoflagellomere is rounded, which is quite a stable character in this species (Figure 11B).
Distribution. Montenegro: Mt Rumija, Greece: Corfu, Mt Olympus.

Description. Size: body length 10-11 mm; wing length 7-8 mm.
Male. Width of face: width of head is 0.28-0.32. Width of vertex: width of the head is 0.19-0.23. Length of eye contiguity: length of frons is 0.28-0.4. Basoflagellomere almost always rounded (Figure 11B). Width of pedicel: width of basoflagellomere is about 0.8. Width of pedicel: length of pedicel is about 0.8. Thorax. Length: width of scutellum is 0.5-0.6.
Female. Width of frons: width of head is 0.27. Width of pedicel: width of basoflagellomere is 0.8. Width of pedicel: length of pedicel is 0.6. Abdomen. Height: width of T4 is 0.7. Height: width of T3 is 0.45.
Etymology. The Phaeacians (Φαίακες, in Gr.), the ancient inhabitants of Corfu Island, were famous for their nautical skills, and renowned for their ability to travel and rapidly reach any location. We selected this name given the origin of the majority of our insect specimens (Corfu) and the wide geographic range of the species.

Taxonomic notes

Doczkal (1996) noted the morphological affinity between *E. minotaurus* and *E. longicornis* and their dissimilarity to *E. niehuisi*, with the latter being morphologically similar and closely related to *E. crassus*. The first two species can be distinguished from the latter two by their slightly shorter body pile, the pruinose supra-alar area without transverse striae, and the scutum without black pile. The pedicels of *E. crassus* and *E. niehuisi* are about 1.5 times as long as deep (Figure 11E), whereas in *E. longicornis* (Figure 11F) and the *E. minotaurus* complex (Figure 11A-C) the pedicel is about twice as long as deep.

New species for the *Eumerus minotaurus* group

Eumerus anatolicus Grković, Vujić and Radenković sp. n.

Type material. Holotype. Male. Turkey: Muğla, University campus (720 m), iv.2011. leg. Kavak. Paratypes. Muğla, University campus (720 m), one female, 17-22.v.2011. legs. Barták and Kubík, 3 males, iv.2011, 2 males, 26.v.-26.vi.2015 leg. Kavak.
Diagnosis. Species belongs to the *E. minotaurus* group and presents the highest similarity to the *E. minotaurus* complex compared to other species of the *E. minotaurus* group, but also displays clear differences to the *E. minotaurus* complex. *E. anatolicus* sp. n. can be distinguished from *E. crassus* and *E. longicornis* by the longer pile on the ventral metatrochanter and metafemur, as well as by the shape of the basoflagellomere (Figure 11D) and the posterior lobe of the surstylus (Figure 10C). *E. anatolicus* sp. n. can be distinguished from the three cryptic species belonging to the *E. minotaurus* complex by patches of grey to white pollinosity on the vertical triangle anteriorly and near the posterior ocelli, as well as by distinctive pollinose maculae on T2-4. In the *E. minotaurus* complex, these markings are linear on T3, whereas in *E. anatolicus* sp. n. they are wider and lunulate. This character is also present in females. Additionally, the vertex of the new species is moderately punctuated and shiny, whereas in the *E. minotaurus* complex it is roughly punctuated and matte. Also, in females of the *E. minotaurus* complex, the frons is wrinkled and covered in white pollinosity along the eye margin apart from an interruption in front of the ocellar triangle, whereas in *E. anatolicus* sp. n., frons is shinier and with a continuous line of pollinosity along the eye margin, as far as the wide pollinose patch behind the posterior ocelli. Regarding the male genitalia, they are very similar to those in the *E. minotaurus* complex but with a slightly larger posterior surstyle lobe and with denser pilosity (Figure 10C) that extends along almost the entire length of the ventral margin (Figure 10F); in species of the *E. minotaurus* complex, this pilosity is restricted to the upper part of the posterior surstyle lobe and sometimes with only a few pile lower down (Figure 10D). The inner lobe of the anterior surstylus is more oval in lateral view than in the *E. minotaurus* complex, covered with fine short pilosity (Figure 10C). The apical part of the aedeagal apodeme is clearly different from those in the *E. minotaurus* complex (Figure 10J).
Distribution. Turkey: Muğla.
Description. Size: body length 10-12 mm; wing length 7-10.5 mm.
Male. Head. Width of face: width of head is 0.30-0.33. Width of vertex: width of head is 0.22-0.24. Length of eye contiguity: length of frons is 0.40-0.47. Eye contiguity 6-10 ommatidia long. Eyes covered in long dense white pilosity, bare near posterior margins. Face, frons, vertex and occiput black with bronze sheen. Face and frons covered in very dense silvery-white pollinosity and white pile. Frons laterally often with a few long black pile mixed with black. Face convex. Vertex and occiput moderately punctuated. Pile on vertex and occiput yellow mixed with black.

Ocelli arranged in an isosceles triangle, longer than wide. Scape and pedicel brown, covered in dense yellow pile, ventrally sometimes longer than the depth of the pedicel. Pedicel elongated, approximately as long as the basoflagellomere and even longer in some specimens (Figure 11D). Width of pedicel: width of basoflagellomere is about 0.9. Width of pedicel: length of pedicel is about 0.7. Basoflagellomere is usually pointed but in some specimens it is oval with the ventral margin quite convex. Thorax. Scutum, scutellum and pleurae black to bronze, densely punctuated. Pleurae, anterior scutum and supra-alar area with fine white pollinosity. Mesonotum with two longitudinal vittae of pollinosity extending up to 4/5 of the length. Narrow median vitta present, almost as long as lateral vittae. Pile on thorax white to yellow. Scutellum roughly striated transversely. Length: width of scutellum is 0.5-0.6. Legs black, tips of femora at both sides brownish. Base of tibiae brownish. Metafemur slightly swollen, ventral pile approximately as long as half the depth of the femur. Metatibia curved in the middle. Wings with dark tinge, entirely microtrichose. Abdomen. Tergites black, densely punctuated and covered in short white pilosity that turns yellow to golden in the posterior half of T4. T2-4 with clearly visible, wide, lunulate maculae of pollinosity. Maculae on T4 narrower. Sternites brown with long white to yellow pile. S4 broad, with yellowish pile posterolaterally. Genitalia. Posterior surstyle lobe large, covered in long, dense and evenly distributed pilosity (Figure 10C). IL covered with short dense pile. Ventral margin of surstylus densely pilose, almost along entire length (Figure 10F).

Female. Similar to the male with normal sexual dimorphism. Head. Width of frons: width of head is 0.3. Frons shiny, moderately punctuated with a continuous line of pollinosity along the eye margin as far as the wide pollinose patch behind the posterior ocelli.